Ⅲ-5

Life, Earth and Planetary Sciences

Highlight

BL4U

Different Distribution of DNA and RNA in Chromosome Revealed by Spectromicroscopy with STXM

A. Ito[1], K. Shinohara[1], H. Yuzawa[2] and T. Ohigashi[2,3]
[1]*School of Engineering, Tokai University, Hiratsuka 259-1292, Japan*
[2]*UVSOR Synchrotron Facility, Institute for Molecular Science, Okazaki 444-8585, Japan*
[3]*SOKENDAI (The Graduate University for Advanced Studies), Okazaki 444-8585, Japan*

Spectromicroscopy using scanning transmission X-ray microscope (STXM) has been applied to study the difference in the distributions of DNA and protein in biological specimens such as chromosome and sperm at the C-K absorption edge [1, 2]. In the previous reports, we developed an image processing procedure for quantitative mapping of biomolecules, and successfully applied to the distribution of DNA and proteins in mammalian chromosomes using combined NEXAFS at the C, N and O-K absorption edges [3, 4].

In the present study, we extended our method to the discrimination of two kinds of nucleic acids, DNA and RNA which have similar chemical composition with slightly different structure: DNA is double-stranded, while RNA is single-stranded. RNA has a uracil base with hydrogen at the 5 position, instead of a thymine base in DNA with a methyl residue at the same position. In addition, DNA is missing an oxygen at the 2' position in a ribose sugar.

Figure 1 shows NEXAFS of DNA and RNA at the C, N and O-K absorption edges by the analysis using aXis 2000 software. Although very similar spectra were obtained as expected, slightly but significantly different profile at the C-K edge was observed.

To discriminate the distribution of such closely related molecules, we introduce the SVD method into the present method. At first, by using the SVD method, relative distributions of DNA, RNA and other molecules including proteins are obtained. The amount of total nucleic acids was estimated from the height of the unique peak of nucleic acids in the NEXAFS at the N-K edge. Quantitative distributions of DNA and RNA with absolute amount were then calculated by distributing the total amount of nucleic acids to each component, DNA and RNA in the images of relative amounts.

We used a chromosome for the discrimination of DNA and RNA. Chromosome was prepared from cultured Chinese Hamster Ovary (CHO) cells as described previously [3].

Figure 2 represents RGB maps that demonstrate the different distribution of DNA (red) and RNA (green). Molecules other than nucleic acids, mainly composed of proteins, are shown by blue.

Interesting observations are as follows:

1) RNA in addition to DNA is also present in chromosomes.

2) RNA distribution was clearly separated from that of DNA. RNA was preferentially located in the outer area of a chromosome.

Detailed analysis was reported recently [5]. These observations should be supported by other methods to detect RNA. The proposed procedure is being successfully applied to RNA distribution in mammalian cells [6], and in apoptotic nuclei [5].

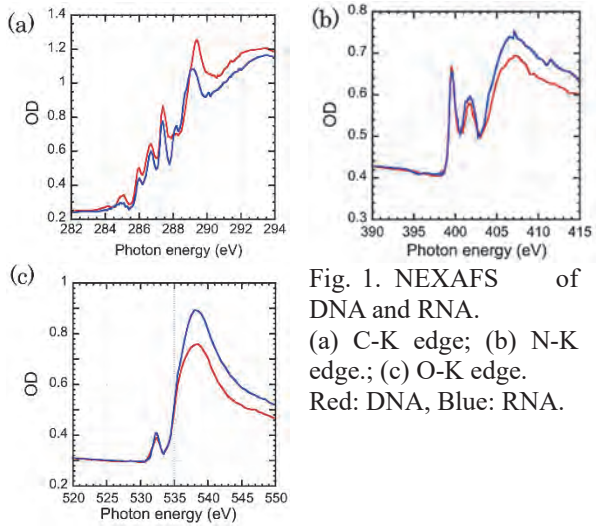

Fig. 1. NEXAFS of DNA and RNA.
(a) C-K edge; (b) N-K edge.; (c) O-K edge.
Red: DNA, Blue: RNA.

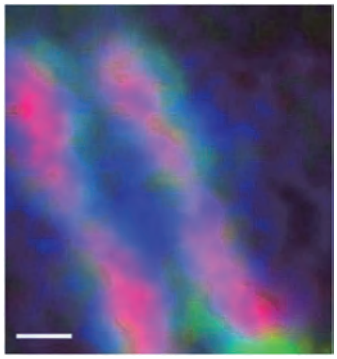

Fig. 2. Distribution of DNA, RNA and other molecules in a CHO chromosome.
Red: DNA; Green: RNA; Other molecules: Blue.
Bar: 0.5 μm

[1] H. Ade *et al*., Science **258** (1992) 972.
[2] X. Zhang *et al*., J. Struct. Biol. **116** (1996) 335.
[3] A. Ito, K. Shinohara, T. Ohigashi, S. Tone, M. Kado, Y. Inagaki and N. Kosugi, UVSOR Activity Report 2017 **45** (2018) 156.
[4] K. Shinohara, T. Ohigashi, S. Tone, M. Kado and A. Ito, Ultramicrosc. **194** (2018) 1.
[5] K. Shinohara, S. Tone, T. Ejima, T. Ohigashi and A. Ito, Cells **8** (2019) 8.
[6] K. Shinohara, A. Ito, T. Ohigashi, M. Kado and S. Tone, J. X-Ray Sci. Technol. **26** (2018) 877.

BL1U

Optical Activity Emergence in Amino-Acid Films by Vacuum-Ultraviolet Circularly-Polarized Light Irradiation (II) - Irradiation Experiments -

J. Takahashi[1], T. Sakamoto[1], Y. Izumi[2], K. Matsuo[2]
M. Fujimoto[3], M. Katoh[3], Y. Kebukawa[1] and K. Kobayashi[1]
[1]*Faculty of Engineering, Yokohama National University, Yokohama 250-8501, Japan*
[2]*Hiroshima Synchrotron Radiation Center, Higashi-Hiroshima 739-0046, Japan*
[3]*UVSOR Synchrotron Facility, Institute for Molecular Science, Okazaki 444-8585, Japan*

The origin of homochirality in terrestrial bioorganic compounds (L-amino acid and D-sugar dominant) remains one of the most mysterious problems in the research for the origins of life. One of the most attractive hypotheses in the context of astrobiology is "Cosmic Scenario" [1] as below.
(1) Prebiotic simple molecules were densely accumulated on interstellar dust surfaces in dense molecular cloud circumstances.
(2) "Chiral radiations" in space induced asymmetric reactions and produced chiral complex organic materials including amino-acid precursors as "chiral seeds".
(3) The "chiral seeds" were transported with meteorites or asteroids to primitive Earth resulting in terrestrial biological homochirality through some kind of "chiral amplification" mechanism.

As for ground experiments to validate the scenario, we already have reported optical activity emergence in solid-phase films of racemic mixture of alanine (DL-alanine) by irradiation of left- or right-handed circularly polarized light (L- or R-CPL). The CPL irradiation experiments were carried out in the air at atmospheric pressure using wavelengths 215 nm from free electron laser (FEL) of UVSOR-II [2] and 230, 215, 203 nm from undulator beamline BL1U of UVSOR-III [3].

We are mainly using circular dichroism (CD) spectroscopy to detect optical activity emergence because CD spectra sensitively reflects the steric structures of chiral molecules with a high degree of accuracy. Theoretical calculation of CD spectrum of alanine molecule has revealed that the circular dichroism chromophores derived from characteristic electronic transitions (n-π*, π-π* for carboxyl group and n-σ*, π-σ* for amino group) are corresponding to several different wavelengths in 120 ~ 230 nm region [4]. From this point of view, it is suggested that the expecting aspects of optical activity emergence by asymmetric photochemical reactions strongly depends on the CPL irradiation wavelength.

We are presently carrying out CPL irradiation experiments using vacuum-ultraviolet (VUV) light at undulator beamline BL1U of UVSOR-III. In case of VUV-CPL irradiation of shorter wavelengths than 200 nm, the DL-alanine film samples were set in a vacuum sample chamber to prevent the attenuation due to photon absorption band by oxygen molecules in the air [5]. On the undulator beam entrance side of the vacuum sample chamber, a gate valve with a vacuum-sealed MgF_2 or LiF window was mounted. The irradiated CPL wavelengths were selected to 180 and 155 nm corresponding to the circular dichroism chromophores of alanine molecule [4].

CD spectra of the CPL irradiated DL-alanine film samples were measured at synchrotron radiation CD beam line BL-12 of Hiroshima Synchrotron Radiation Center (HiSOR) to clarify the optical activity emergence by the CPL irradiation. Preferential structural changes between the two enantiomers in racemic amino-acid mixtures introduced by the CPL irradiation can be detected by using CD spectroscopy. In Fig. 1, CD spectra of DL-alanine films after irradiation with L- and R-CPL at 180 nm (Fig.1(a)) and 155 nm (Fig.1(b)) in wavelength are shown. Detailed analysis of CD spectra are in progress to clarify full mechanism of the optical activity emergence, which potentially has relevance to the origin of terrestrial bioorganic homochirality stimulated by "chiral radiation".

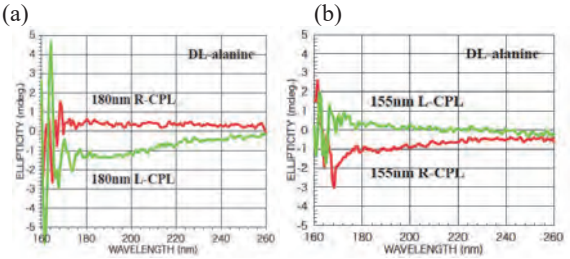

Fig. 1. CD spectra of the L- or R-CPL irradiated DL-alanine films measured at BL-12 of HiSOR. The CPL irradiation wavelengths were (a) 180 nm and (b) 155 nm at BL1U of UVSOR-III.

[1] W. A. Bonner, Orig. Life Evol. Biosph. **21** (1991) 407.
[2] J. Takahashi *et al.*, Int. J. Mol. Sci. **10** (2009) 3044.
[3] K. Matsuo *et al.*, UVSOR Activity Report 2016 **44** (2017) 157.
[4]F. Kaneko *et al.*, J. Phys. Soc. Jpn. **78** (2009) 013001.
[5] J. Takahashi *et al.*, UVSOR Activity Report 2017 **45** (2018) 147.

BL2B

Impacts of Ambient Conditions on the Electronic States of a Molecular Semiconductor Bis(1,2,5-thiadiazolo)-*p*-quinobis(1,3-dithiole)

Y. Nakayama[1], K. Sudo[1] and Y. Watanabe[2]
[1]*Department of Pure and Applied Chemistry, Tokyo University of Science, Noda 278-8510, Japan*
[2]*Department of Mechanical and Electrical Engineering, Suwa University of Science, Chino 391-0292, Japan*

Bis(1,2,5-thiadiazolo)-*p*-quinobis(1,3-dithiole) (BTQBT) is a promising molecular material for organic electronics applications because of its widely dispersed intermolecular valence bands in the crystalline thin films [1] and good performance in use of vertical field effect transistor devices [2]. On the other hand, the degradation under the ambient conditions has been a common problem for the organic semiconductor materials. In this study, evolution of the electronic states of BTQBT thin films grown on Au substrate were tracked before and after exposure to ambient conditions by means of photoelectron spectroscopy (PES).

BTQBT was deposited on Au-coated Si substrates in ultra-high vacuum conditions. PES measurements were conducted at BL2B, UVSOR, by using an electron spectrometer R3000 (VG-Scienta). The photon energy was fixed at 120 eV in this work. All measurements were done at room temperature.

Figure 1 shows PES spectra of the Au substrate and 10 nm-thick BTQBT film plotted together with a simulated density-of-states (DOS) curve being expected from a molecular orbital energy distribution derived from quantum chemical calculation. This suggests that, whereas the spectral profiles of the present BTQBT film have to be regarded as superposition of the DOS of BTQBT and signals from the Au substrate, at least the highest-occupied molecular orbital (HOMO)-derived component of BTQBT can be separated from the 5d bands of Au.

Evolution of the BTQBT HOMO-derived PES peak and work function upon exposure to the ambient conditions is shown in Figs. 2(a) and 2(b), respectively. While the energy positions of the HOMO and vacuum level were substantially unchanged in ultra-high vacuum (10^{-7} Pa) condition for more than one month, an exposure of the BTQBT film to the ambient air in dark only for 5 minutes brought about a significant (ca. 0.2 eV) decrease and increase in the hole injection barrier and work function, respectively. Further exposure induced extra spectral shifts in the same direction. Interestingly, additional exposure to air with the ambient light made a change in the opposite direction, i.e., increase in the hole injection barrier and decrease in the work function. This implies a possibility that the presence/absence of the ambient light may lead to different degradation paths of the BTQBT-based electronic devices.

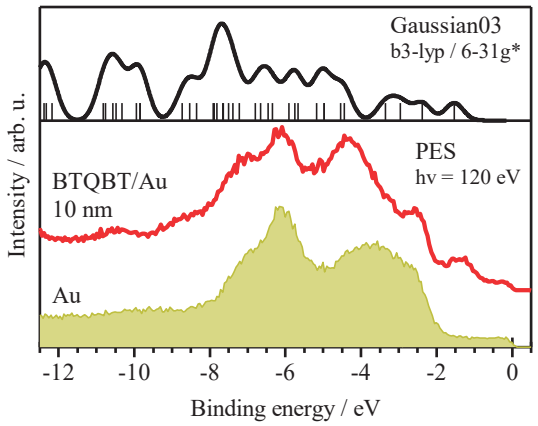

Fig. 1. PES spectra of the Au substrate (orange) and BTQBT film (red). A simulated DOS curve derived from the calculated molecular orbital pattern (vertical bars) is also displayed in the upper panel.

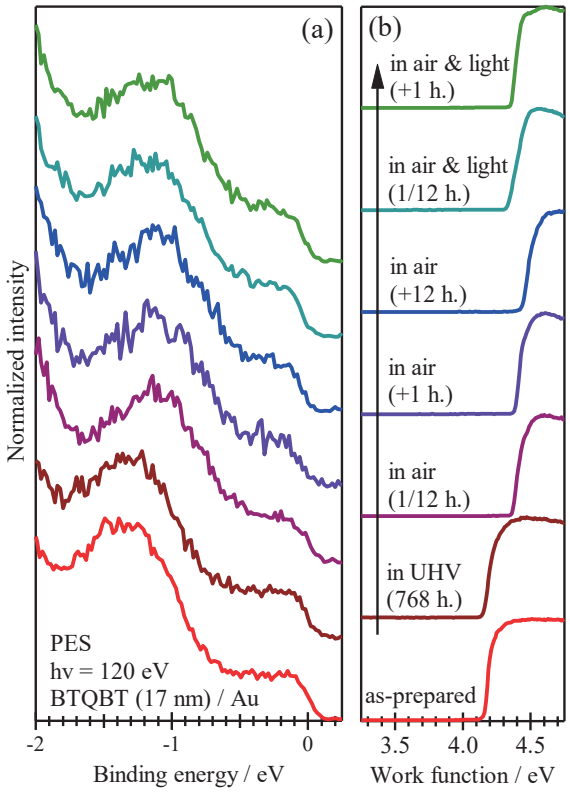

Fig. 2. Evolution of the PES spectra in the (a) HOMO and (b) secondary electron cutoff regions of the 17 nm-thick BTQBT induced by the ambient exposure.

[1] S. Hasegawa *et al.*, J. Chem. Phys. **100** (1994) 6969.
[2] H. Fukagawa *et al.*, AIP Adv. **6** (2016) 045010.

BL3U

X-ray Absorption Spectroscopy Measurement of Lipid Bilayer Membranes in Aqueous Solutions

R. Tero[1], S. Nakamura[1], Y. Sano[1] and M. Nagasaka[2]
[1]*Toyohashi University of Technology, Toyohashi, 441-8580, Japan*
[2]*Institute for Molecular Science, Okazaki 444-8585, Japan*

The lipid bilayer is a self-assembled structure of amphiphilic lipid molecules, and is the fundamental structure of biomembranes such as cell membranes. Lipid bilayer provides reaction fields for transporting materials, information and energy into and out of cells. Internal structures of lipid bilayers, e.g. two dimensional domains and hydrophobic thickness, and physical properties affect the transportation reactions. All these physiological reactions proceeds in the presence of ions. Ions in the aqueous solution significantly influence to these structures and properties of lipid bilayers. Phosphatidylcholine (PC) (Fig. 1) is the major component of eukaryotic cells. Cations bind to the phosphate and carbonyl groups of PC. However, affinity of cations to PC, and also other lipids, are still controversy especially in the fields of theoretical simulations [1]. In this study, we aim to determine the binding affinity of cations to the phosphate and carbonyl groups experimentally. This year we started X-ray absorption spectroscopy (XAS) measurement of a PC bilayer in aqueous solution, to detect the chemical shifts of O 1s binding energy.

We prepared a suspension of dioleoyl-PC (DOPC) vesicles in a buffer solution using a tip-type sonicator. We introduced the suspension into the XAS flow cell consisting of Si_3N_4 membranes [2]. Planar DOPC bilayers were formed on the Si_3N_4 membranes (Fig. 2) through the process of vesicle fusion method [3]. Fluorescence microscope imaging and fluorescence recovery after photobleaching method showed that the Si_3N_4 membranes were fully covered with planar DOPC bilayers.

Figure 3 shows an O K-edge spectrum the Si_3N_4 membrane flow cell with DOPC bilayers on its inner surface. We improved the experimental, and obtained a peak comprising of several components at 530-533 eV. It was isolated from the peaks of bulk water, which appeared above 533 eV. The components were attributed to the phosphate and carbonyl groups of DOPC, and to the native oxide layer on Si_3N_4. After subtracting the blank spectrum of Si_3N_4 without the DOPC bilayer, we found that at least two O 1s components originating from PC, and also that from molecular oxygen that was dissolved in the hydrophobic core of the bilayer membrane. The DOPC bilayer existed stably after repeated solution exchange. We showed that O K-edge spectra of lipid bilayers can be measured in aqueous solution the XAS flow cell. Next year we will measure PCs without phosphate or carbonyl groups, to identify the PC-originated peaks.

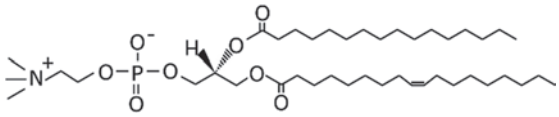

Fig. 1. Molecular structure of a representative phosphatidylcholine.

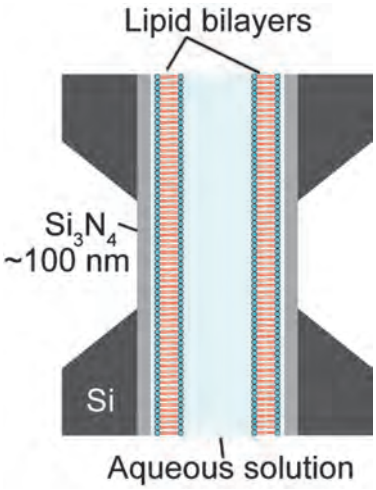

Fig. 2. Schematic of a lipid bilayer sample in the flow cell for XAS measurement.

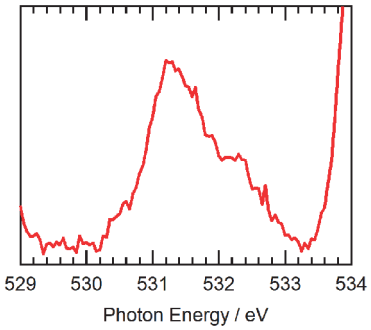

Fig. 3. O K-edge spectrum in absorbance of the Si_3N_4 membrane covered with a DOPC planar bilayer.

[1] T. B. Woolf, Biophys. J. **104** (2013) 746.
[2] M. Nagasaka, H. Yuzawa, T. Horigome and N. Kosugi, J. Electron Spectros. Relat. Phenomena **224** (2018) 93.
[3] R. Tero, Materials **5** (2012) 2658.

BL3U

Study of Micelle Formation in Aqueous Solutions of Fatty Acids Using Soft X-ray Absorption Spectroscopy

J. J. Lin[1], G. Michailoudi[1], R. R. Kamal[1], H. Yuzawa[2], M. Nagasaka[3,4] and N. L. Prisle[1]

[1]*Nano and Molecular Systems research unit, University of Oulu, P.O. Box 3000, 90014 University of Oulu, Finland*

[2]*UVSOR Synchrotron Facility, Institute for Molecular Science, Okazaki 444-8585, Japan*

[3]*Institute for Molecular Science, Okazaki 444-8585, Japan*

[4]*School of Physical Sciences, The Graduate University for Advanced Studies (SOKENDAI), Okazaki 444-8585, Japan*

Atmospheric aerosols have a key role in global climate as they interact with solar radiation and take part in cloud formation [1]. Fatty acids and their salts are found both in urban and marine environments, and are well-known surfactants, meaning that they accumulate at the liquid/gas interface, including that of water droplets in the atmosphere. With a hydrophilic head (carboxyl group) and a hydrophobic tail (aliphatic chain), surface active molecules can form films on the surface of an aqueous solution, with the heads oriented towards the water. Above the critical micelle concentration (CMC), these molecules can self-assemble into structures called micelles, which in turn can impact both chemical and physical properties of the solutions, including surface tension which play an important role in cloud microphysics [2, 3].

At BL3U, we studied binary systems of fatty acids in aqueous solutions and also ternary water–fatty acid–salt solutions with varying concentrations above and below the respective CMC values, using X-ray absorption spectroscopy (XAS) on a liquid flow cell [4]. XAS is highly sensitive to the chemical environment of different components in solution and provide information about the bulk properties of dissolved compounds.

The studied liquid samples were aqueous solutions of sodium hexanoate ($C_5H_{11}COONa$) at 0.75, 1, 2, 3, 4 and 5 CMC (CMC = 0.9 M) and ternary solutions of sodium hexanoate and sodium chloride salt (H_2O–$C_5H_{11}COONa$–NaCl) at 5.3 M of NaCl and approximately 1.5 times the ternary CMC for $C_7H_{15}COONa$. This value is not well-know and basing the concentration on a multiple of CMC involves estimating the dependency of CMC on solution salt content. Spectra of pure hexanoic acid ($C_5H_{11}COOH$) and aqueous $C_5H_{11}COOH$ solution (7.3 M) were also measured as a reference.

The thickness of the liquid cell was optimized for better absorption and the sample temperature was set at 25°C. We monitored solution properties of surfactant molecules and their micelle formation by scanning the C *K*-edge from 280 to 300 eV, in energy steps of 0.02 eV from 285 to 290 eV and 0.1 eV for the remainder of the range.

Figure 1 presents a preliminary analysis at the C *K*-edge XAS spectra for binary and ternary solutions, after normalization at the peak position. A background spectrum of absorption from water was subtracted, removing also signal from carbon contamination on the liquid cell membranes. Solutions with highest concentration resemble the pure acid. Furthermore, the ratio of the pre-peak feature to main peak changes with the concentration of the surfactant relative to the CMC. From such changes and energy shifts on peak position of our spectra, we expect to extract information about the structures present in each solution.

Further analysis is needed to fully interpret the spectra, including an appropriate fitting procedure and identifying underlying peaks from the occurring excitations in the C *K*-edge from comparison to theoretical predictions. Model predictions for these and similar systems are the focus of ongoing work.

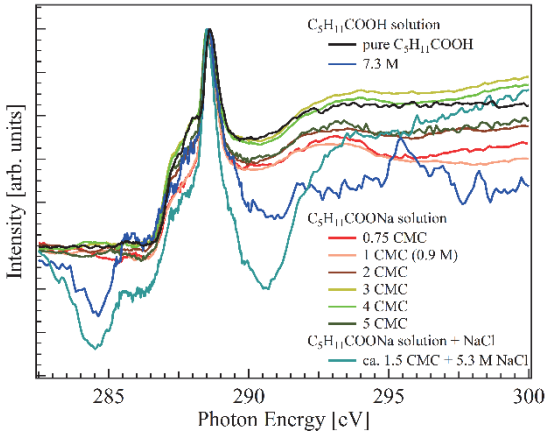

Fig. 1. C *K*-edge XAS spectra of pure $C_5H_{11}COOH$, aqueous $C_5H_{11}COOH$ and aqueous $C_5H_{11}COONa$ solutions at various multiples of the CMC value, and of H_2O–$C_7H_{15}COONa$–NaCl ternary solution.

[1] Intergovernmental Panel on Climate Change: *Climate Change 2013: The Physical Science Basis,* Cambridge University Press, New York, USA, 2013.
[2] P.S. Gill *et al.*, Rev. Geophys. **21** (1983) 903.
[3] M.C. Facchini *et al.*, Atmos. Environ. **34** (2000) 4853.
[4] M. Nagasaka *et al.*, J. Electron Spectrosc. Relat. Phenom. **224** (2018) 93.

BL4U

Estimation of the Thickness of Fe(III)-oxides Layer near the Magnetite (111) Surface after Hydrothermal Treatment

T. Tamura, A. Kyono and I. Kinebuchi

Division of Earth Evolution Sciences, Graduate School of Life and Environmental Sciences, University of Tsukuba, Tsukuba 305-8572, Japan

Since the discovery of hydrothermal chimneys and black smoker vents in 1979 [1], a great variety of hydrothermal vents has been found all over the world [2-4]. Some of them are characterized by hydrothermal fluids enriched in molecular hydrogen (H_2) [5]. Previous studies have shown that the hydrogen generation can be induced by water-magnetite interaction [6, 7]. Furthermore, it has been reported that the reaction is accompanied by oxidation of magnetite (Fe_3O_4) to maghemite (γ–Fe_2O_3) [7], but the mechanism has been still unknown. In the study, we employed a scanning transmission X-ray microscopy (STXM) to estimate the thickness of maghemite layer.

About 0.02 g of synthesized magnetite crystals were introduced into the 28 ml Teflon–lined stainless steel autoclave. Ultrapure water was in advance sufficiently bubbled with N_2 gas to remove dissolved O_2. 14 ml of the deoxidized water were added into the Teflon container. The autoclave was tightly sealed and then heated at 200 °C for 24 hours. After the hydrothermal treatment, the magnetite crystals were removed from the Teflon container and dried at room temperature. After amorphous carbon was deposited on the sample surface, a cross–section was prepared with a JEOL JEM–9320FIB focused ion beam (FIB) system using a 30 keV Ga ion source. The FIB cross–section was analyzed using a STXM at UVSOR branch line 4U.

The Fe L_{23} edges provide chemical information about valence-specific multiplet structures of iron which can be used as valence fingerprints. In the study, the Fe L_3 and L_2 edges were clearly observed at around 709 and 722 eV, respectively (Fig. 1). The L_3 edge shape obtained at a depth of 100 nm seemed to be split, which suggesting that hematite is formed at the surface. With increasing the depth, the split peaks of L_3 edge were merged into one broad peak. The Fe L_2 edge peaks at 721.0 and 722.5 eV were, on the other hand, continuously observed up to a depth of 800 nm, but a new peak at 721.5 eV became dominant from 900 nm (Fig. 1). The result implies that maghemite (γ-Fe_2O_3) is dominantly distributed between 100 nm and 800 nm. Therefore, we can conclude that during hydrothermal reaction magnetite is oxidized to hematite through maghemite.

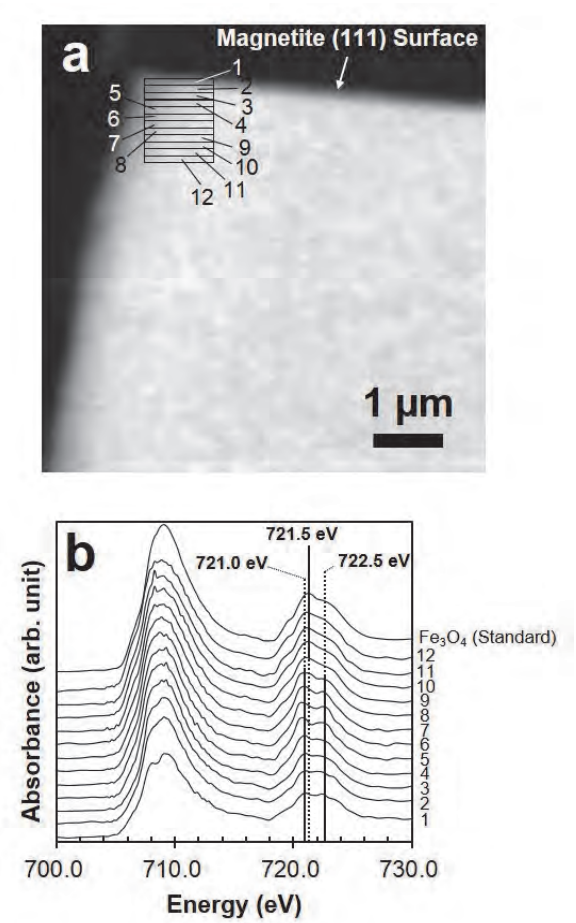

Fig. 1 (a) Fe distribution map of cross-section perpendicular to hydrothermally treated (111) magnetite surface. The box size is 100 nm of depth. (b) Fe L_{23} edge XANES spectra of hydrothermally treated magnetite resulting from the image stack on the area depicted in (a). Reference spectra of as grown magnetite is also shown for comparison.

[1] Corliss *et al.*, Science **203** (1979) 1073.
[2] Hekinian *et al.*, Science **219** (1983) 1321.
[3] Azuende *et al.*, J. Geophys. Res. **101** (1996) 17995.
[4] Connelly *et al.*, Nat. Commun. **620** (2012) 1.
[5] Kelley *et al.*, Science **307** (2005) 1428.
[6] Mayhew *et al.*, Nat Geosci. **6** (2013) 478.
[7] Tamura *et al.*, J. Mineral. Petrol. Sci. **113** (2018) 310.
[8] Almeida *et al.*, Nat. Commun. **5154** (2014) 1.

BL4U

Investigating the Effect of Space Exposure Experiment on Carbonaceous Dust Based on XANES/STXM Analysis

I. Sakon[1], I. Endo[1], H. Yabuta[2] and T. Noguchi[3]
[1]*Department of Astronomy, Graduate School of Science, University of Tokyo, Tokyo 113-0033, Japan*
[2]*Graduate School of Science, Hiroshima University, Higashi-Hiroshima 739-8526, Japan*
[3]*Division for Experimental Natural Science, Faculty of Arts and Science, Kyushu University, Fukuoka 819-0395, Japan*

We have carried out the space exposure experiment of various kinds of carbonaceous solids using International Space Station (ISS) Japanese Experiment Module 'Kibo' ExHAM (See the top panel of Fig. 1). The major goal of this project is to understand how the carbonaceous dust particles synthesized in the stellar ejecta from evolved stars are chemically and physically altered in nature in the circumstellar environment until it becomes a member of the interstellar medium. In particular, we aim to investigate the properties of 'astronomical' polycyclic aromatic hydrocarbons (PAHs), the carrier of the unidentified infrared (UIR) bands, which have been observed ubiquitously in various astrophysical environments [1]. So far, we have brought three experiment samples to the ISS. Each experiment sample has a 10cm x 10cm exposure surface and has 64 slots for exposure experiment materials. In total, more than 40 kinds of materials including filmy quenched carbonaceous composites (filmy-QCCs [2]), nitrogen-included carbonaceous composites (NCCs [3]), anthracite, graphite, and silicates are installed in the experiment samples. Among the three samples, two of them (EE64-I and EE64-II) were attached on ExHAM-1 and were exposed in the space exposure environment for 384 days from 26 May 2015 to 13 June 2016. The final sample (EE64-III) was attached on ExHAM-1 and was exposed for 386 days from 29 June 2016 to 19 July 2017. All the samples are now collected back on earth and the difference in properties of our exposure experiment materials between before and after the experiment is investigated based on infrared micro-spectroscopy.

The bottom panel of Fig. 1 shows the comparison of the infrared spectra of the filmy-QCC before and after the experiment. In addition to the presence of new features at 2.95 μm, attributed to O-H stretching with moderate hydrogen-bonding, and at 5.95 μm, attributed to C=O stretching of conjugated ketone and/or aldehyde, a broad bump structure in 8-10 μm has been recognized. In order to identify the effect of space exposure on the filmy-QCC, we have carried out the XANES/STXM analyses of TEM samples made by FIB processing of filmy-QCC (U-02 in EE64-I) and non-exposed filmy-QCC as a reference.

Our beamtime using the BL4U STXM beamline of the UVSOR was scheduled on July 24-25 in 2018, however, we still have not yet obtained the conclusive results of the XANES/STXM measurement due to beam trouble that has happened in July 2018. We have proposed an another try in this semester (first half of 2019) and the beamtime was allocated in this June and July.

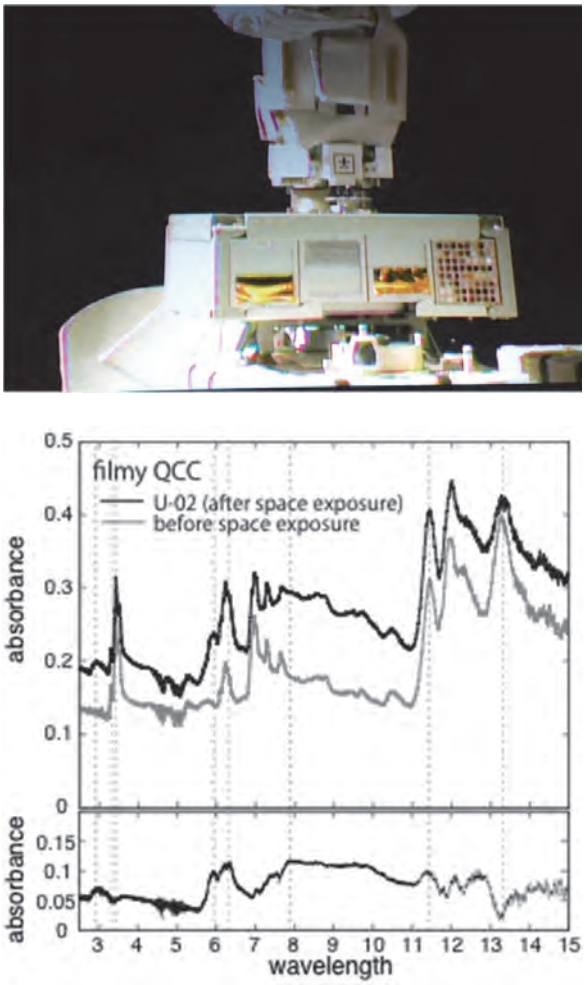

Fig. 1. [Top] A photo of space exposure experiment of EE64-I and EE64-II attached to ExHAM (credit: JAXA/NAXA), [Bottom] The comparison of the infrared spectra of the filmy-QCC before and after the space exposure experiment.

[1] A. T. Tokunaga, ASP Conf. Ser. **124** (1997) 149.
[2] A. Sakata *et al*., Nature **301** (1983) 493.
[3] I. Sakon *et al*., Asian Journal of Physics **24** (2015) 1143.

BL4U

Investigation of Origin and Evolution of Organic Material inside the Extraterrestrial Material with a Series of in-situ Analyses: Construction of System for the Inter-facility Collaboration for the Analysis of Hayabusa2 Returned Samples

M. Uesugi[1], M. Ito[2], K. Tomioka[2], Y. Kodama[3], T. Ohigashi[4,5], H. Yuzawa[4], K. Uesugi[1], A. Yamaguchi[6], N. Imae[6], Y. Karouji[7], N. Shirai[8], T. Yada[9] and M. Abe[9]

[1]*Japan synchrotron radiation research institute (JASRI/SPring-8), Sayo 679-5198, Japan*
[2]*Kochi Institute for Core Sample Research, Japan Agency for Marine-Earth Science Technology (JAMSTEC), Nankoku 783-8502, Japan*
[3]*Marine Works Japan Ltd., Yokosuka 237-0063, Japan*
[4]*UVSOR Synchrotron Facility, Institute for Molecular Science, Okazaki 444-8585, Japan*
[5]*School of Physical Sciences, The Graduate University for Advanced Studies (SOKENDAI), Okazaki 444-8585, Japan*
[6]*Antarctic Meteorite Research Center, National Institute of Polar Research, Tachikawa 190-8518, Japan*
[7]*Space Exploration Innovation Hub Center, Japan Aerospace Exploration Agency (JAXA), Sagamihara 252-5210, Japan*
[8]*Department of Chemistry, Graduate School of Science, Tokyo Metropolitan University, Hachioji 192-0397, Japan*
[9]*Institute of Space and Astronautical Science, Japan Aerospace Exploration Agency (JAXA), Sagamihara 252-5210, Japan*

Hayabusa2 spacecraft successfully touched down on the surface of asteroid Ryugu, in Feb. 2019. It is scheduled that the spacecraft will return back to the Earth in 2020, with the sample of Ryugu [1]. Reflectance spectrum of the surface of Ryugu suggested that the sample would have water and carbonaceous materials, those similar to carbonaceous chondrites found on the Earth.

We started the development of techniques and devices for the handling, transfer and analysis of samples returned by Hayabusa2 spacecraft from 2015, by organizing a special team constituting of members of Japan Aerospace Exploration Agency (JAXA), Japan Agency for Marine-Earth Science and Technology (JAMSTEC), Institute for Molecular Sciences (IMS), SPring-8 and National Institute of Polar Research (NIPR) [2]. The team, called Phase 2 team Kochi, will also analyze the Hayabusa2 returned samples from 2021.

Rehearsal of the analysis of Hayabusa2 returned samples was started in 2017 using Antarctic micro-meteorites (AMMs) which simulated the small returned particles. 10 AMMs, with diameter around 100μm, provided by NIPR were observed by synchrotron radiation computed tomography (SR-CT) and x-ray diffraction (XRD) at SPring-8, high resolution field emission scanning electron microscopy and energy dispersive spectroscopy (FE-SEM-EDS) system at IMS. Through the series of non-destructive analysis, we selected two AMMs those having characteristics similar to carbonaceous chondrites, and extracted thin sections by focused ion beam (FIB) for the analysis of organic materials by scanning transmitted x-ray microscopy and x-ray absorption near edge structure (STXM-XANES) at BL4U.

We found two different phases of organic matter in AMMs, spotty particles with high carbon density and broad distribution of organics with low density of carbon, in C-XANES analysis. They also show different C-XANES spectrum, suggesting different origin or evolutional history. Though spatial resolution is not enough to resolve precise structure of those phases, high resolution analysis by transmission electron microscopy (TEM) at JAMSTEC revealed that the spotty particles are hollow organic globules (HOG) those are previously reported by literatures [3][4]. However, the number density of the HOG is almost ten times higher than previous result obtained by TEM [3]. This means that wide-area observation of organics by STXM-XANES, with spatial resolution less around 0.1 μm, is important for analysis of extraterrestrial organic material, and also characterization of parent extraterrestrial material.

In future works, we will examine other extraterrestrial materials, such as hydrated and/or heated carbonaceous chondrites with same manner.

[1] S. Tachibana *et al*., Geochemical Journal **48** (2014) 571.
[2] M. Ito *et al*., LPSC conf. (2019) abstract#1394.
[3] K. Nakamura-Messenger *et al*., Int. J. Astrobiol. **1** (2002) 179.
[4] L.A. Garvie, P. R. Buseck Earth. Planet. Sci. Lett. **224** (2004) 431.

BL4U

Aqueous Alteration Scenario in Martian Meteorite Based on Chemical Speciation

N. Shiraishi[1], H. Suga[1], M. Miyahara[1], T. Ohigashi[2], Y. Inagaki[2], A. Yamaguchi[3], N. Tomioka[4], Y. Kodama[5] and E. Ohtani[6]

[1]*Department of Earth and Planetary Systems Science, Graduate School of Science, Hiroshima University, Higashi-Hiroshima 739-8526, Japan*

[2]*UVSOR Synchrotron Facility, Institute for Molecular Science, Okazaki 444-8585, Japan*

[3]*National Institute of Polar Research, Tokyo 190-8518, Japan*

[4]*Kochi Institute for Core Sample Research, Japan Agency for Marine-Earth Science and Technology, Nankoku 783-8502, Japan*

[5]*Marine Works Japan, Nankoku 783-8502, Japan*

[6]*Department of Earth Sciences, Graduate School of Science, Tohoku University, Sendai 980-8578, Japan.*

Previous studies showed that Martian meteorite clan nakhlite has evidence for a rock-fluid reaction occurred on the Mars. One of the representative fingerprints for the rock-fluid reaction is “iddingsite”, which is the alteration texture formed in and around the olivine grains of nakhlites. Iddingsite is the assemblages of any kinds of secondary minerals. The mineral species, compositions, and chemical species of the iddingsite depend on the varied parameters such as temperature and pH of the fluid contributing to the reaction [e.g., 1]. Accordingly, the secondary minerals in the iddingsite allow us to elucidate the physicochemical properties of the fluid in ancient Martian subsurface and its origin.

In this study, we clarified the mineral species, chemical compositions, and chemical species of the secondary minerals in the iddingsite of the nakhlite Yamato 000749 (Y 000749) using a combined SEM-Raman-FIB-TEM-STXM technique. In particular, FIB-STXM measurement is a unique point of this study. We performed two-dimensional chemical state analysis using X-ray absorption near edge structure (XANES).

TEM images revealed that the iddingsite in Y 000749 had a layer structure (oxidized olivine: laihunite–ferrihydrite–low crystalline silica minerals in Fig. 1a). Fe-XANES spectra revealed that most irons in the original olivine and iddingsite were divalent and trivalent, respectively (Fig. 1b). Based on O-XANES spectra (Fig. 1c) and TEM observations, most of the iron oxides in the iddingsite of Y000749 were identified as ferrihydrite. In addition, S-XANES spectra and TEM observations revealed that a small amount of iron sulfate mineral coexisted with ferrihydrite.

On the basis of the occurrences and formation conditions of the secondary minerals, we expect that Y 000749 experienced three different alteration events at least. The alteration of Y000749 was initiated by the formation of ferrihydrite subsequent to the formation of laihunite, which occurred under high-temperature and high-pH conditions [2]. Then, silicon dissolved in the fluid precipitated as low-crystalline silica minerals. Thus, by combining the FIB-STXM analysis of secondary minerals with the conventional model calculations, we can disclose more detailed environmental evolution processes on Mars.

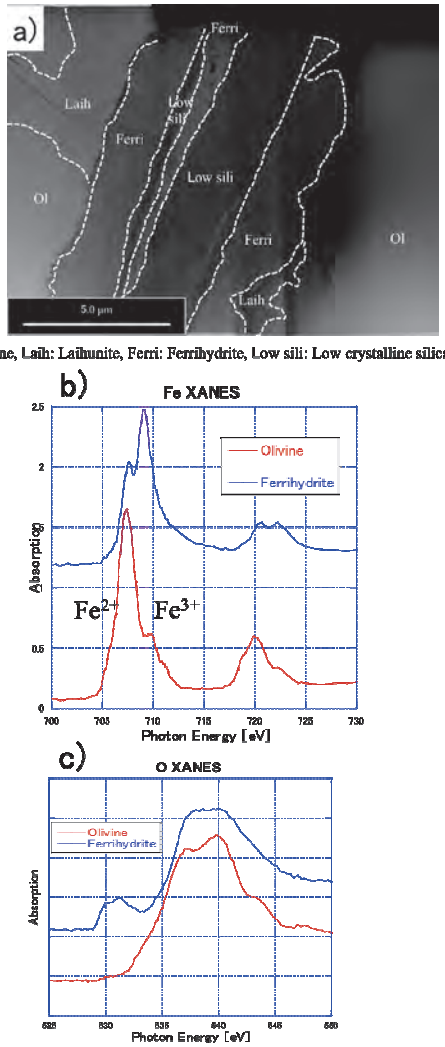

Fig. 1. a) HAADF-STEM image, b) Fe-XANES, c) O-XANES of the iddingsite in Y 000749.

[1] Bridges J.C. and Grady M.M., Earth Planet. Sci. Lett. **176** (2000) 267.
[2] Treiman A.H., Chem Erde-Geochem **65** (2005) 203.

BL4U

Sulfur Map in Organics in Meteorites by STXM-XANES and NanoSIMS

M. Ito[1], R. Nakada[1], H. Suga[2], T. Ohigashi[3], Y. Kodama[4] and H. Naraoka[5]
[1] *Kochi Inst. for Core Sample Res., JAMSTEC, Nankoku 783-0086, Japan*
[2] *The University of Tokyo, Tokyo 113-8654, Japan*
[3] *UVSOR Synchrotron Facility, Institute for Molecular Science, Okazaki 444-8585, Japan*
[4] *Marine Works Japan, Yokosuka, 237-0063, Japan*
[5] *The Kyushu University, Fukuoka, 812-0053, Japan*

Organic matter in carbonaceous chondrites is composed of an insoluble macromolecule (aka insoluble organic matter: IOM) and complex soluble organic molecules (OM). The total organic content is around 4 wt% in chondrites (IOM of ~75 wt%) [1]. The proposed composition of IOM is $C_{100}H_{70}O_{22}N_3S_7$ [1] or $C_{100}H_{48}N_{1.8}O_{12}S_2$ [2].

The STXM studies were carried out to identify functional groups of C, N and O in organics of extraterrestrial materials (IOM in chondrites [3], cometary returned sample [4], organics in Hayabusa Category-3 particles [5], organics in IDPs [6], and organics extracted from halite in the Monahans LL chondrite [7]). However, sulfur study by XANES in the extraterrestrial organics is very rare [8, 9].

In our experiments at Inst. Mole Sci. UVSOR synchrotron BL4U, we have reported nine sulfur L_3-edge spectra from sulfur bearing terrestrial organics; sodium lauryl sulfate, sodium methanesulfonate, dibenzothiophene, thianthrene, DL-methionie, DL-methionine sulfone, L-cysteic acid, L-cystein, and L-cystine showing different absorption curves (e.g., sulfate, sulfone, thiol) [10].

In this study, we report preliminary results of sulfur speciation measurements by S-XANES in the FIB sections of the Murchison and the Tagish Lake meteorites using scanning transmission X-ray microscope (STXM) at the BL4U. The purpose of this study is understanding of sulfur speciation, its distribution and isotopic compositions ($^{33}S/^{32}S$, $^{34}S/^{32}S$, $^{36}S/^{32}S$) within organics in a carbonaceous chondrite which may provide the secondary alteration processes of thermal metamorphism and aqueous alteration in the parent body.

We successfully obtained high resolution S-STXM image of FIB sections from the Murchison (147 x 187 pixels, 22 x 28 μm^2: spatial resolution = 150 nm) and the Tagish Lake meteorites (01L section = 132 x 132 pixels, 33 x 33 μm^2 and spatial resolution = 250 nm). Figure 1a shows S-STXM (Red: 173.6 eV assigned to sulfate) image together with IOM (Green) and diffused OM (Blue) images in the Murchison FIB section. Figure 1b is a representative S-XANES spectra in the Murchison FIB section. First and second strong peaks in Fig. 1b may be related to sulfate based on our previous sulfur L_3-edge spectra for organic standards [10]. We might find small peak around 181 eV which assigned to sulfonate in Fig. 1b, and difficult to assign 164 eV peak which is related to organic sulfide. The S-STXM spectra of Tagish Lake is slightly different peaks and peak-top shape. We found several μm-sized spots having the S-STXM spectra in the Tagish Lake section.

We, then, conducted S (red), C (green), and O (blue) elemental imaging with the JAMSTEC NanoSIMS for the Murchison FIB section in comparison with the STXM image (red: Sulfate, green: IOM, blue: DiffOM) of the same FIB section (Fig. 2). Note that the green area in both images are almost identical each other implying NanoSIMS C-image are relate to the IOM. However, S regions from both sections show completely different locations within the entire section. S distributions observed by STXM is an organic component, but S image obtained by NanoSIMS might be inorganic components (i.e., FeS).

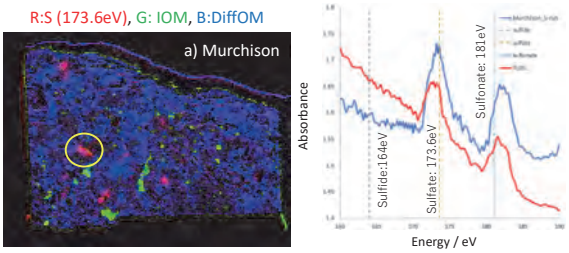

Figure 1. a) STXM image of Murchison FIB section, and b) S-XANES spectra of the Murchison and Tagish Lake meteorites

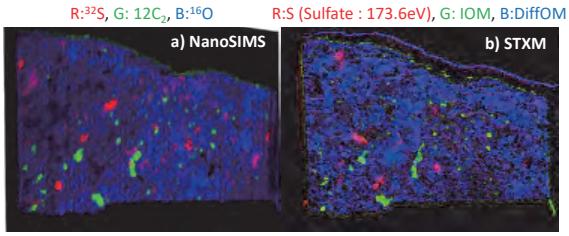

Figure 2. Comparison a) NanoSIMS elemental image and b) STXM image

[1] Remusat, EPJ Web of Conferences **18** (2011) 05002.
[2] Gilmour, In Meteorit., comets and planets, Treatise on Geochemistry, (2005) 269.
[3] Kebukawa *et al*. 2019. Scientific Reports, **9**:3169.
[4] Sanford *et al.,* Science **314** (2006) 1720.
[5] Yabuta *et al.,*. EPS **66** (2014) 156.
[6] Flynn *et al.,* Geochim Cosmochim Acta **67** (2003) 4791.
[7] Chan *et al*,. Science Advance **4** (2018) eaao3521.
[8] Orthous-Daunay *et al*., EPSL **300** (2010) 321.
[9] Bose *et al*., Meteor Planet Sci. **52** (2017) 546.
[10] Ito *et al.,* UVSOR activity report 2017 **45** (2018) 84.

BL4U

Hyperspectral Imaging by Scanning X-ray Microscopy: Probing the Penetration of Rapamycin in Fixed Human Skin

G. Germer[1], T. Ohigashi[2], H. Yuzawa[2], F. Rancan[3], A. Vogt[3] and E. Rühl[1]
[1]*Physical Chemistry, Freie Universität Berlin, Arnimallee 22, 14195 Berlin, Germany*
[2]*UVSOR Synchrotron Facility, Institute for Molecular Science, Okazaki 444-8585, Japan*
[3]*Charité Universitätsmedizin, 10117 Berlin, Germany*

Progress in hyperspectral imaging using scanning X-ray microscopy is reported. This is facilitated by using a custom-made Ni-coated zone plate for investigations in the O 1s-regime, which provides higher photon flux and improved spatial resolution compared to previous beam times. This substantial improvement allowed us to take for fixed human skin sample stacks of images, which cover multiple photon energies in the O 1s regime (520 – 560 eV, 134 energy steps) in areas of a size of 20 µm x 5 µm with 100 nm step width as well as high resolution maps with 30 nm step width (size: 4 µm x 2 µm). This provides substantially more detailed information than in our previous work, where X-ray micrographs were taken at a few pre-selected photon energies [1]. These were chosen according to characteristic changes in absorption of the species under study, allowing for determining the location of the penetrating drug. The present developments go beyond, so that the spectral shapes in the near-edge regime as well as their differences can also be used for identifying highly dilute species in a given compartment of biological matter. This is of importance for identifying local changes induced by topical drug delivery. We have investigated for the first time the skin penetration of the anti-inflammatory drug rapamycin (sirolimus) ($C_{51}H_{79}NO_{13}$, M=914.13 g/mol), a well-known mTOR inhibitor. Skin penetration of rapamycin is expected to be inefficient due to its high molecular mass [2], if not properly formulated. The present studies were performed at the O 1s-edge, where the drug is selectively probed at the O 1s→π*-resonance near 531 eV, which is characteristically shifted in energy compared to the matrix of fixed human skin. The skin was partially treated before drug penetration by serine protease [3], enhancing the drug penetration. This was verified for rapamycin dissolved in ethanol, where the drug was only observed in the stratum corneum in the lipophilic membranes between the corneocytes after long penetration times, reaching up to 1000 min (see Fig. 1). In contrast, intact skin samples do not provide evidence for such drug penetration, underscoring the successful use of primary serine protease treatment as a prerequisite for drug penetration. Figure 1(a) shows a high resolution micrograph of such skin sample. Clearly visible is the stratified structure of the stratum corneum (SC). Distinct changes in local composition are visible at the locations A and B. The raw spectra (Fig. 1(b)) show only minor differences in shape, but when the contribution of a reference skin sample is subtracted (see Fig. (1c)), then evidence is found for the local abundance of rapamycin (location A), whereas in corneocytes (location B) only enhanced intensity in the O 1s continuum is observed (see Fig. 1(c)). This progress will be systematically exploited for subsequent studies involving redox nanocarriers for bringing the drug efficiently in viable skin layers.

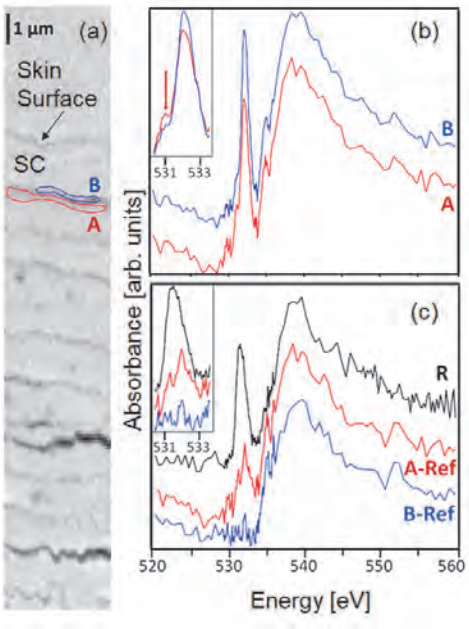

Fig. 1. (a) X-ray micrograph of fixed human skin treated with serine protease and subsequently exposed for 1000 min with rapamycin (R), SC: stratum corneum, A: lipophic lamella; B: corneoyte; (b) X-ray absorption spectra at the locations A and B at the O 1s-edge; (c) reference spectrum of rapamycin and at the locations A and B subtracted by the contribution of reference skin (A-Ref; B-Ref). The insets in (b) and (c) show the O 1s→π*-bands in greater detail.

[1] K. Yamamoto *et al.*, Anal. Chem. **87** (2015) 6173; Eur. J. Pharm. Biopharm. **118** (2017) 30; Eur. J. Pharm. Biopharm. **139** (2019) 68.
[2] J. D. Bos *et al.*, Exp. Dermatol. **9** (2000) 165.
[3] J. Frombach *et al.*, Z. Phys. Chem. **232** (2018) 919.

BL4U

Ultrastructural Features in Mice Liver Samples Imaged Using STXM

M. Patanen[1,2], H. Yuzawa[3], T. Ohigashi[3], T. Mansikkala[1,2], I. Miinalainen[2], S. M. Kangas[2,4], A. E. Hiltunen[2,4], E.-V. Immonen[1,4], R. Hinttala[2,4], J. Uusimaa[2,4], N. Kosugi[3] and M. Huttula[1]

[1]*Nano and Molecular Systems Research Unit, PO Box 3000, 90014 University of Oulu, Finland*
[2] *Biocenter Oulu, PO Box 5000, 90014 University of Oulu, Finland*
[3]*UVSOR Synchrotron Facility, Institute for Molecular Science, Okazaki 444-8585, Japan*
[4]*PEDEGO Research Unit and Medical Research Center Oulu, and Oulu University Hospital, PO Box 5000, 90014 University of Oulu, Finland*

In this work, we have used scanning transmission X-ray microscopy (STXM) technique at BL4U beamline to study liver tissue samples of control (healthy) mice and mice with a mutation in *NHLRC2* gene. The *NHLRC2* gene encodes an NHL repeat containing protein 2 ubiquitously present in various types of tissues, from animals to bacteria. Recently, we have characterized a novel, fatal cerebropulmonary disease in children with fibrosis, neurodegeneration and cerebral angiomatosis (FINCA disease) [1]. FINCA disease has been linked to mutations in *NHLRC2*, but the functional role of the *NHLRC2* is still unknown. Transmission Electron Microscopy (TEM) images of analysis of immortalized cell cultures from FINCA patients demonstrated multi lamellar bodies and distinctly organized vimentin filaments, and based on thorough multitechnique characterization, it was suggested that *NHLRC2* dysfunction enhances tissue fibrosis [2]. Previously, we have also reported an STXM study of human FINCA patient tissue samples which were in line with TEM results [3].

Recently, we have created a knock-in mouse model for FINCA disease utilizing the CRISPR-Cas9 technology. This mouse model enables us to investigate the changes in ultrastructural features as the disease progresses. For the present study, liver sections from control mice and knock-in mice were collected from 13 weeks old mice. Tissue samples were fixed in 4% paraformaldehyde and 2.5% glutaraldehyde in 0.1 M phosphate-buffered saline. Prior to embedding in resin some samples were stained with 1% OsO_4 and/or uranyl acetate. Some samples were left without staining in order to investigate its effects. The 100 nm thick sections of resin-embedded sample were measured first with STXM, and then further imaged at Biocenter Oulu using a Tecnai G2 Spirit 120kV TEM (FEI, Eindhoven, The Netherlands) equipped with a Quemesa CCD camera (Olympus Soft Imaging Solutions GmbH, Münster, Germany).

Figure 1 shows examples of a FINCA mouse liver section without block staining imaged with STXM and after with TEM. Radiation damage seems to thin the sample, as the STXM imaged regions are clearly visible as lighter regions in TEM images. However, no ultrastructural changes in sample due to radiation were observed. The average STXM image taken over the O K-edge is presented in optical density, in contrast to transmission mode of TEM images. A cluster analysis of STXM image stacks (Figs. 1c & f) was performed using a MANTiS software [4]. Even with the resin-embedded unstained samples, the cluster analysis was able to differentiate cell components rather consistently based on their spectral information. For example, the Figs. 1b-d contain a cell nucleus with a nucleolus, which the cluster analysis also catches, and in Fig. 1f mitochondria (orange) are well separated from the surrounding endoplasmic reticulum (green). The result shows great promise in ultrastructural characterization of unstained tissue samples using STXM.

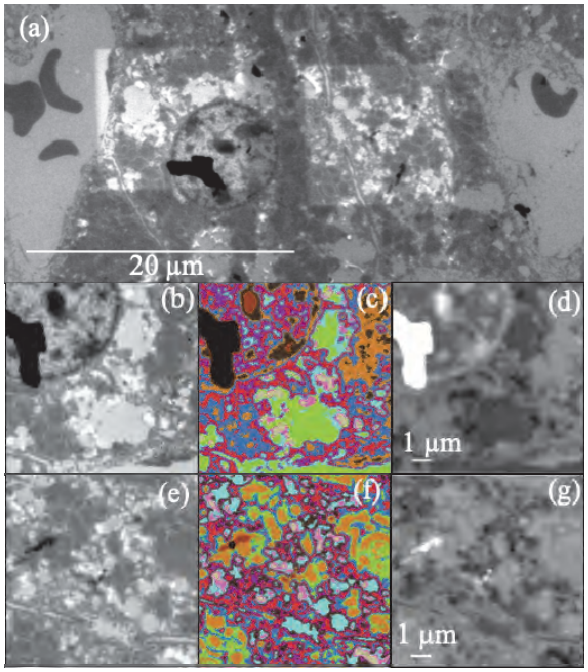

Fig. 1. (a) TEM image of the FINCA mouse sample studied after STXM. (b) & (e) Higher resolution TEM images of the studied areas. (c) & (f) Cluster analysis of the STXM image stacks. (d) & (g) Average STXM image recorded over O K-edge.

[1] J. Uusimaa *et al*., Acta Neuropathol. **135** (2018) 727.
[2] T. Paakkola *et al*., Hum. Mol. Gen. **27** (2018) 4288.
[3] E.-V. Immonen *et al.,* UVSOR Activity Report 2017 **45** (2018) 161.
[4] M. Lerotic *et al*., J. Synchr. Rad. **21** (2014) 1206.

BL4U

The Molecular Structures and Distributions of Organic Matter Depending on the Lithologies of the Tagish Lake Meteorite Examined by C- and Fe-XANES

K. Kiryu[1], Y. Kebukawa[2], T. Ohigashi[3] and K. Kobayashi[2]
[1]*Graduate School of Engineering Science, Yokohama National University, Yokohama 240-8501, Japan*
[2]*Faculty of Engineering, Yokohama National University, Yokohama 240-8501, Japan*
[3]*UVSOR Synchrotron Facility, Institute for Molecular Science, Okazaki 444-8585, Japan*

The Tagish Lake meteorite is an anomalous carbonaceous chondrite (CC) and contains abundant organic matter (OM) which has been affected by aqueous alteration in the parent bodies [1]. In the process of aqueous alteration, specific minerals may be involved in the reaction of OM. In fact, the distributions of OM overlap with these of phyllosilicates and partially carbonates in Tagish Lake [2]. Phyllosilicates are known to adsorb OM [e.g., 3], and thus they possibly serve as catalysts of the reactions of OM [e.g., 4, 5]. Tagish Lake is known to consist of various lithologies [1, 6]. Therefore, we aim to evaluate the relationships between minerals and OM through microscopic analyses of various lithologies of the Tagish Lake meteorite.

Fragments from three different lithologies of Tagish Lake ("Pristine", "KN2", and "Degraded" samples) were observed using a scanning electron microscope (SEM) and energy dispersive X-ray spectroscopy (EDS). We selected four areas randomly and two areas based on the EDS (a Mg-rich region and a carbonate region). Six ultrathin sections (~100 nm thick) were prepared using focused ion beam (FIB). We analyzed these sections by scanning transmission X-ray microscope (STXM) and obtained C- and Fe-X-ray absorption near-edge structure (XANES) from C-rich regions in the FIB sections. The C-XANES spectra of Tagish Lake showed peaks at 287.3 eV (aliphatic C), 285.2 eV (aromatic C), 288.5 eV (carboxyl and/or ester) and 290.3 eV (carbonate) (Fig. 1), and the Fe-XANES spectra showed peaks at 706.8 eV (Fe^{2+}) and 708.5 eV (Fe^{3+}) (Fig. 2).

To compare molecular structures of OM in various fragments from Tagish Lake, C-XANES peak intensities were normalized to the intensity at 291.5 eV (ionization potential). The normalized intensities of aliphatic C were KN2 (carbonate region) > Pristine ≥ KN2 (Mg-rich region) > KN2 > Degraded. The Fe^{2+}/Fe^{3+} ratios were lower in the OM rich regions compared to the OM poor regions. These results indicate that the molecular structure of OM varies among lithologies of Tagish Lake, possibly related to chemical compositions of coexisting minerals.

Acknowledgements: We thank Dr. M. E. Zolensky and Dr. W. Fujiya for providing the Tagish Lake meteorite samples, and Dr. M. Ito for preparing the FIB sections.

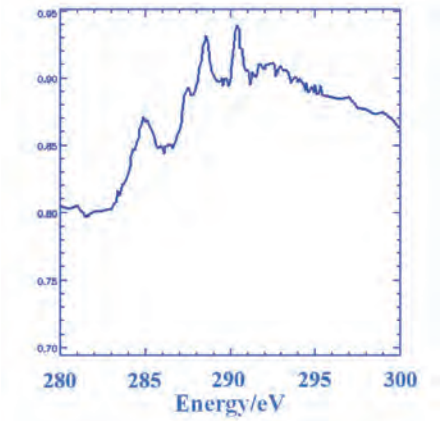

Fig. 1. C-XANES obtained from a FIB section of Tagish Lake "KN2".

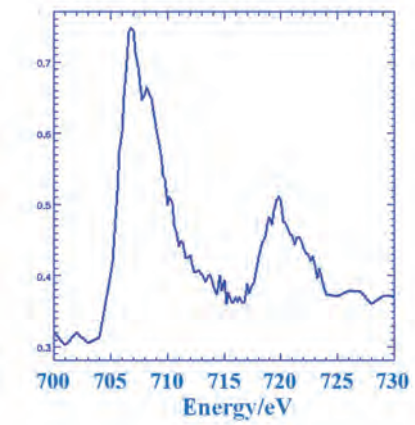

Fig. 2. Fe-XANES obtained from a FIB section of Tagish Lake "KN2" (same region to Fig. 1).

[1] C. D. K. Herd *et al.*, Science **332** (2011) 1304.
[2] M. Yesiltas and Y. Kebukawa, Meteoritics & Planetary Science **51** (2016) 584.
[3] M. Kahle *et al.*, Organic Geochemistry **35** (2004) 269.
[4] L. B. Williams *et al*, Geology **33** (2005) 913.
[5] J. S. Watson and M. A. Sephton, Astrobiology **15** (2015) 787.
[6] M. E. Zolensky *et al.*, Meteoritics & Planetary Science **37** (2002) 737.

BL4U

Composition of Carbon Functional Group of Soil Organic Matter in Clay Size Fraction in Initial Forming Stage of Volcanic Ash Soils in Japan

M. Asano [1], V. F. Eseese [2], H. Shimada [2], K. Tamura [1] and T. Ohigashi [3,4]

[1]*Fuculty of Life and Environmental Sciences, University of Tsukuba, Tsukuba 305-8572, Japan*
[2]*Graduate School of Life and Environmental Sciences, University of Tsukuba, Tsukuba 305-8572, Japan*
[3]*UVSOR Synchrotron Facility, Institute for Molecular Science, Okazaki 444-8585, Japan*
[4]*School of Physical Sciences, The Graduate University for Advanced Studies (SOKENDAI), Okazaki 444-8585, Japan*

Soil is the largest terrestrial carbon reservoir in the World. Soil organic matter (SOM) accounts for a major portion of terrestrial C and is considered to be stabilized against microbial degradation due partly to its interaction with soil minerals. These organo-mineral interactions contribute to the formation of heterogeneous organo-mineral particles at various space scales down to submicron level [1]. Volcanic ash soil tend to accumulate large amounts of carbon as SOM in comparison to other soil type. The abundance of Short Range Order minerals and secondary Al, Fe and Si–humus complexes are common in developed volcanic ash soil (Andosols) which contributes to its SOM accumulation capacity [2]. On the other hand, the changing of organo-mineral interactions with weathering process on fresh volcanic ash during soil forming is remain unclear. The research on initial soil forming process on fresh volcanic ash under natural environment is important to understand the development of Andosols and carbon dynamics in volcanic region.

Here we focused on the carbon functional groups within the organo-mineral particle in the initial soil forming stages using scanning transmission X-ray microscopy (STXM) and near-edge X-ray absorption fine structure (NEXAFS) at UVSOR BL4U. We compared top soil from different soil ages, immature volcanic ash soil (Regosol) and mature volcanic ash soil (Andosol). The smaller than 2 μm fraction was separated by particle size fractionation method [3].

The C-NEXAFS spectrum of organo-mineral particles showed clear difference between Regosol and Andosol. To show the C chemical composition map, we split the C K-edge spectra three energy regions, 284–286 eV (aromatic C), 286–287 eV (phenol and aliphatic C), and 287–289 eV (amid and carboxyl C) (Figs. 1 and 2). The C functional group map of Regosol was dominated by carboxylic C with minimal Aliphatic C and Aromatic C (Fig. 1). The C functional group map of Andosol shows also dominated by carboxyl C, but Aromatic C and Aliphatic C appeared clear than Regosol (Fig. 2). Those results indicated amide and carboxylic C, potentially labile C, was accumulated in both immature and mature soils.

We will further examine microstructure, diffraction pattern, and elemental composition of specific regions within the tested organo-mineral particles in this report by transmission electron microscope (TEM) to discuss organo-mineral interactions.

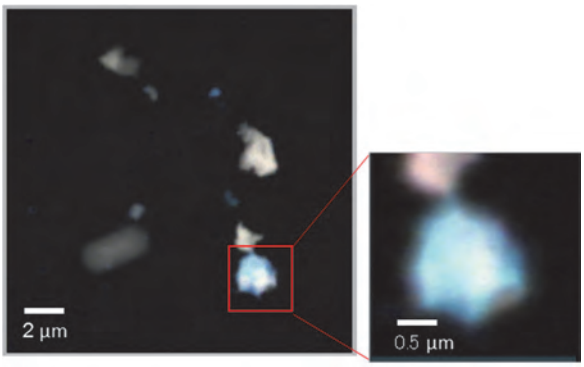

Fig. 1. Carbon functional group map of immature soil (Regosol). red: 284–286eV (aromatic C), blue: 286–287 eV (phenol and aliphatic C), and green: 287–289 eV (amide and carboxyl C).

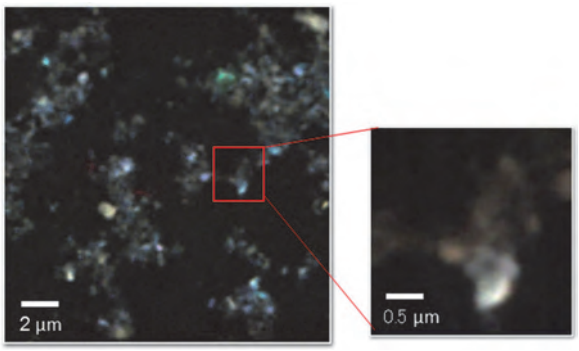

Fig. 2. Carbon functional group map of mature soil (Andosol). red: 284–286eV (aromatic C), blue: 286–287 eV (phenol and aliphatic C), and green: 287–289 eV (amide and carboxyl C).

[1] M. Asano *et al*., Soil Systems **2** (2018) 32.
[2] R. A. Dahlgren *et al*., Adv. Agron. **82** (2004) 113.
[3] M. Asano and R. Wagai, Geoderma **216** (2014) 62.

BL4U

STXM-XANES Analysis of Carbonaceous Matter in ~3.95 Billion-year-old Sedimentary Rocks

M. Igisu[1], T. Ohigashi[2,3], H. Yuzawa[2] and T. Komiya[4]

[1]*Department of Subsurface Geobiological Analysis and Research, Japan Agency for Marine-Earth Science and Technology (JAMSTEC), Yokosuka 237-0061, Japan*

[2]*UVSOR Synchrotron Facility, Institute for Molecular Science, Okazaki 444-8585, Japan*

[3]*School of Physical Sciences, The Graduate University for Advanced Studies (SOKENDAI), Okazaki 444-8585, Japan*

[4]*Department of Earth Science and Astronomy, The University of Tokyo, Meguro 153-8902, Japan*

Carbonaceous matter (CM) in Archean (approximately 4-2.5 billion years ago) sedimentary rocks provides important insights into understanding the physiological and phylogenetic characteristics of life on early Earth [1]. The presence of life on Earth has been inferred primarily from morphologically preserved microscopic fossils, stromatolites, molecular biomarkers, and stable isotopic compositions in sedimentary rocks. Recently, ^{13}C-depleted CM was found in ~3.95 billion-year-old metasedimentary rocks in Labrador, Canada, which provides the oldest evidence of life on Earth [2]. The carbon isotopic signatures provide potential chemical evidence of microbial activity in the environment at the time. However, they do not necessarily offer clues for distinguishing whether the products are derived from the microbial functions of the bacterial and/or archaeal populations. In this study, we characterized the molecular structure of CM in order to obtain insights into its origin.

The C-K and N-K X-ray absorption near edge structure (XANES) spectra of CM in sedimentary rocks were acquired using a scanning transmission X-ray microscope (STXM) at the BL4U, UVSOR. Analyzed sedimentary rocks were a pelitic rock (LAF497) and a conglomerate (LAD849A), both containing CM. Before XANES analyses, Raman microspectroscopic analysis was performed on the petrographic thin sections to identify the presence of CM and examine its graphitization degree [3]. The Raman spectra revealed that the CM in the pelitic rock was less graphitized as compared to that in the conglomerate. Thin cross-sectional foils (about 100-150 nm thick) containing CM were then prepared by focused ion beam (FIB) milling for thin sections of both peltic and conglomerate rocks.

Figure 1 shows an example of a C-XANES spectrum of the CM in the conglomerate. Absorption peaks at 285 eV and at 292 eV correspond to 1s → π* of electronic transitions in aromatic C=C bonds, and 1s → σ* exciton of graphite, which are typical for graphitized carbon [4]. The CM in the pelitic rock has similar C-XANES spectra to that in the conglomerate, regardless of the difference in their graphitization degrees. N-XANES spectra for the CM did not exhibit clear absorption peaks. Figure 2 reveals submicron-scaled heterogeneity of carbon within one CM grain. Although one possible explanation for this heterogeneity is the orientation of the graphite layer, further examination of the microstructure of the CM is required for further validation.

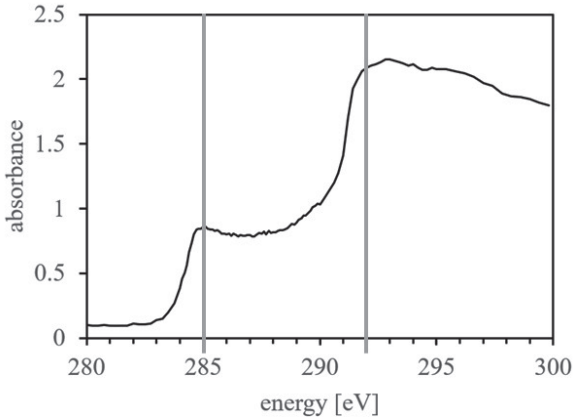

Fig. 1. Carbon-XANES spectrum of the CM (LAD849A).

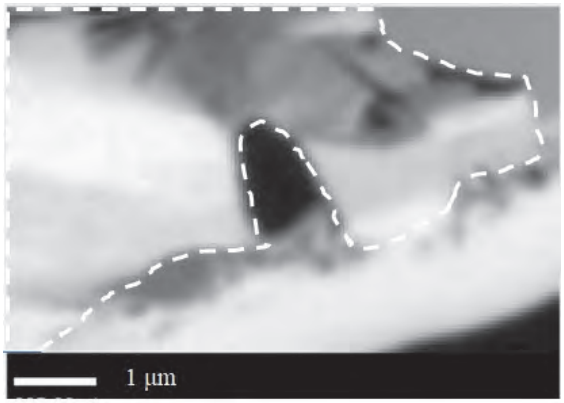

Fig. 2. A STXM image at 285 eV of the analyzed foil (LAD849A).

[1] J. J. Brocks, Emerging Topics in Life Sciences **2** (2018) 181.
[2] T. Tashiro *et al*., Nature **549** (2017) 516.
[3] O. Beyssac *et al*., J. Metamorph. Geol. **20** (2002) 859.
[4] G. D. Cody *et al*., Earth Planet. Sci. Lett. **272** (2008) 446.

BL4U

3-Dimensional Spectroscopy of an Isolated Cell Nucleus by Using a Scanning Transmission X-ray Microscope

T. Ohigashi[1,2], H. Yuzawa[1], S. Toné[3], K. Shinohara[4] and A. Ito[4]
[1]*UVSOR Synchrotron Facility, Institute for Molecular Science, Okazaki 444-8585, Japan*
[2]*School of Physical Sciences, The Graduate University for Advanced Studies (SOKENDAI), Okazaki 444-8585, Japan*
[3]*Graduate School of Advanced Science and Technology, Tokyo Denki University, Hatoyama 350-0394, Japan*
[4]*School of Engineering, Tokai University, Hiratsuka 259-1292, Japan*

Apoptosis is a programmed cell death which is frequently observed in many biological processes such as developmental process. Then, nuclear condensation and DNA fragmentation occur during process of apoptosis, and this process is classified into 3 stages regarding to morphology of nucleus. Apoptosis is generally observed by using fluorescence microscope with staining process but high resolution image, chemical compositions and 3-dimensional (3D) structure of apoptosis are still unclear. Then, scanning transmission X-ray microscopy (STXM) with computer tomography (CT) is a promising tool to elucidate these issues with 3-dimensional (3D) distribution of chemical states. In the previous report, we performed STXM-CT of an isolated cell nucleus at N K-edge since DNA and protein have remarkable spectral features at N K-edge [1]. However, qualities of 3D distributions of DNA and protein were not good mainly due to saturation of X-ray absorption [2]. In this report, we tried STXM-CT of the cell nucleus by using O *K*-edge.

The isolated cell nucleus of HeLa S3 cell at stage 0 (i.e. a normal cell) was used as a sample. After fixation by glutaraldehyde, the cell nucleus was performed critical point drying. The cell nucleus was glued on a tip of a tungsten needle (TP-005, Micro Support Co., Ltd.) with a crystal bond and the tungsten needle was fixed on a CT sample cell [3]. As data acquisition, 50 image stacks, each of which is consisted of 48 STXM images around O *K*-edge region from 528 to 538 eV, were obtained manually with rotating the sample 3.6° each (in total 180° rotation) to obtain complete projection data. Their measurement conditions are as follows; scan area is 8×8 μm^2 composed of 50×50 pixels, and the dwell time is 1s per a pixel. This measurement condition was determined to keep radiation damage on the sample minimum.

As a pre-process of reconstruction, position shifts in the image stacks were aligned and were converted to optical density (OD) images by using aXis2000 program. By extracting the OD images of same energies from each image stack, sinograms were obtained. Cross-sectional images were reconstructed from these sinograms by home-made filtered-back projection algorithm.

3D reconstructed image (volume projection by using ImageJ software) and, for an example, a cross sectional image of the isolated cell nucleus at the X-ray energy of 528 eV are shown in Fig. 1. With noticing structures of nucleoli and filaments, X-ray absorption spectra are extracted from the areas in Fig. 1b (Fig. 2). Peaks of π* resonance of the spectra (around 532 eV) resemble those of DNA and protein in their position and shape.

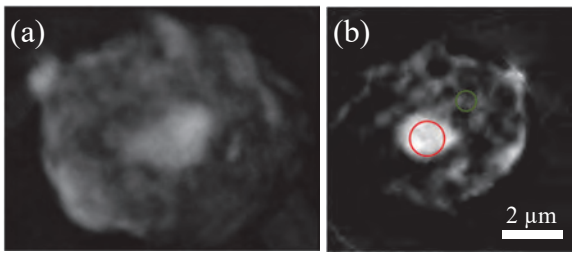

Fig. 1. (a) 3D volume projection image and (b) a cross sectional image of the isolated cell nucleus of the X-ray energy of 528 eV.

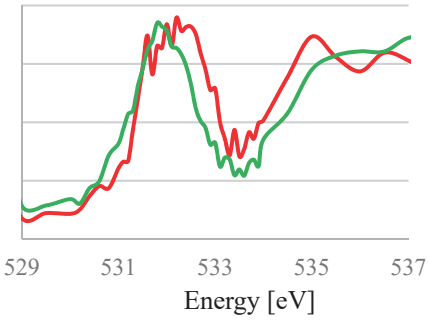

Fig. 2. Spectra extracted from reconstructed energy stack. Colors of the spectra correspond to the areas indicated in Fig. 1(b).

[1] T. Ohigashi, A. Ito, K. Shinohara, S. Tone, M. Kado, Y. Inagaki, Y-F. Wang and N. Kosugi, AIP Conf. Proc. **1696** (2016) 020027.
[2] T. Ohigashi, A. Ito, K. Shinohara, S. Toné, Y. Inagaki, H. Yuzawa and N. Kosugi, Microsc. Microanal. **24** (2018) 400.
[3] T. Ohigashi, Y. Inagaki, A. Ito, K. Shinohara and N. Kosugi, J. Phys.: Conf. Ser. **849** (2017) 012044.

BL4U

Study on the Mechanism of Microbial Weathering of Oceanic Crust by in situ Observation of the Basalt-cell Interface

S. Mitsunobu, S. Urano and J. Fukudo
Department of Agriculture, Ehime University, Matsuyama 790-8566, Japan

The weathering of oceanic basalts is one of the most crucial water-rock interaction ubiquitously occurring in the vast oceanic crust. The weathering of oceanic basalt has a significant impact on Earth's climate on a geological timescale by providing a sink for atmospheric CO_2 through carbonization of oceanic basalts [1]. The fresh basalt rock contains abundant Fe (about 10 wt.%) and its major species is ferrous iron (Fe(II)) and initial $Fe(II)/Fe_{total}$ ratio in fresh basalt ranges between 82 and 90% [2]. Hence, when the oceanic basalts are exposed to oxidative conditions, the Fe(II) in basalts is gradually oxidized to Fe(III) in the weathering process on a geological timescale even at low temperature in deep seafloor [3]. Recent previous studies have reported that oceanic microorganisms (mainly bacteria) would play a significant role to the oxidation of Fe(II) in the basalt. Also, it is indicated that bacterial Fe(II) oxidation would promote the whole weathering process of oceanic crust [3], as the rate of microbial Fe(II) oxidation is generally more rapid than that of chemical oxidation by dissolved O_2. There have been considerable efforts to investigate chemical and biological mechanism of the oxidation of Fe(II) involved in the oceanic basalt. However, little is known on the mechanism of microbial Fe(II) in the basalt alteration, because direct chemical speciations of Fe and biomolecules at rock-microbe interface has been difficult due to a short of spatial resolution in the analysis.

Here, we examined the mechanisms of the Fe(II) oxidation in basalt weathering by using direct scanning transmission X-ray microscopy (STXM)-based NEXAFS analyses at UVSOR BL4U. The basalt sample used in the study was prepared by in situ incubation of fresh basalt glass for 12 months at deep seafloor (water depth: 700-800 m) in Izu-Ogasawara bonin.

STXM-based merged Fe/C image and C 1s NEXAFS were shown in Fig. 1. The NEXAFS clearly showed that the spectrum obtained at bacterial cell-basalt interface (area 3) in the incubated basalt glass contains a strong peak corresponding for acidic polysaccharides (alginate), addition to the other biomolecules of protein, DNA, and lipid. The spectral features were not observed in those of whole cell area. These finding indicates that the sessile bacteria attached on the basalt glass largely produced the polysaccharide-rich extracellular polymeric substances at the cell-basalt interface. The biogenic polysaccharides are likely to form a strong complex with Fe(II) under wide pH region [3]. Thus, our finding from C NEXAFS analysis suggests that the sessile bacteria produce the polysaccharides on the basalt glass to enhance the dissolution of basalt by the complexation between the cell and basalt surface. These findings would be an important knowledge to understand mechanism of bacteriogenic weathering of oceanic crust.

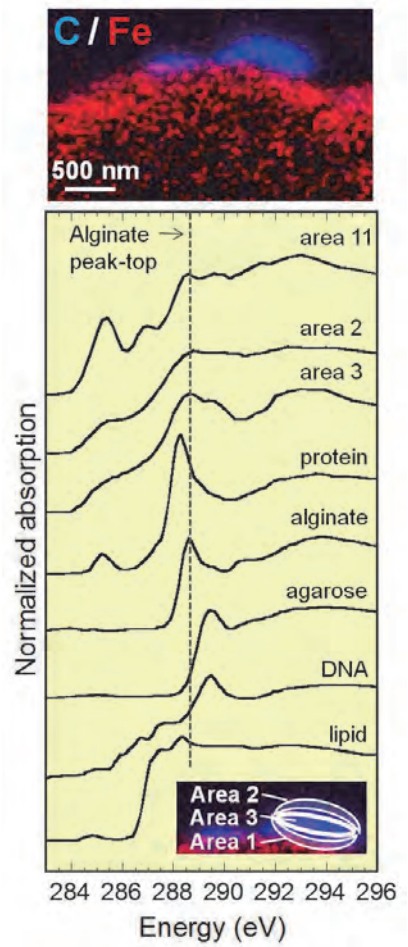

Fig. 1. STXM-based C and Fe images (upper) and C 1s NEXAFS spectra (bottom).

[1] H. Staugigel *et al.*, Geochim. Cosmochim. Acta **53** (1989) 3091.
[2] A. Bezos and E. Humler, Geochim. Cosmochim. Acta **69** (2005) 711.
[3] W. Bach and K.J. Edwards, Geochim. Cosmochim. Acta **67** (2003) 3871.

BL4U

Chemical Mapping of Individual Atmospheric Nanoparticles

R. R. Kamal[1], J. J. Lin[1], G. Michailoudi[1], H. Yuzawa[2], T. Ohigashi[2] and N. L. Prisle[1]
[1]*Nano and Molecular Systems Research Unit, University of Oulu, Oulu 90041, Finland*
[2]*UVSOR Synchrotron Facility, Institute for Molecular Science, Okazaki 444-8585, Japan*

Chemical maps were drawn for three types of aerosol samples. 1) Laboratory-generated aerosols with 150 nm diameter, produced by atomization of solutions of sodium n-decanoate and sodium chloride with different mixing ratios. 2) Urban aerosol samples collected in Beijing during a winter campaign from October 2017 to January 2018 jointly operated by Peking University and the University of Gothenburg. Sampling was carried out at the Peking University Atmosphere Environment Monitoring Station on the roof of a six-floor building on the campus of Peking University located in the northwestern urban area of Beijing. A SKC 4-stage cascade impactor was used to collect particles with cut-off sizes of 250 and 500 nm that were impacted onto Formvar films. 3) Plastic reference samples prepared from industrial grade plastics sliced as thinly as possible to ensure good transmission of X-rays. Slices were made of 100 and 60 nm polyethylene and 150 and 100 nm polypropylene using microtome. Spectra are to our knowledge first of their kind and will serve as reference for characterizing microplastic collected in nature.

Based on chemical formula, plastic samples should only contain C-C bonds, and the absorption region from 280 to 320 eV was studied. Along with uniform presence of expected C-C, as seen in selected region of Fig 1 (a), plastic samples also showed presence of K^+ group. Occurrence of K was only around the sample edges, indicating potential contamination during cutting and slicing of the plastics. The spectrum in (c) also shows a small peak at 285 eV corresponding to C=C [1], and further analysis is required to confirm what contributes to that peak.

The urban aerosol samples were examined at the absorption edges of carbon, nitrogen, sulfur, silicon, chlorine, calcium, iron, vanadium, and titanium, to identify their possible origins from e.g. organic sources, mineral dust, or traffic emission. Figure 2 shows the optical density of one particle probed at the carbon (a), sulfur (b), and calcium (c) edges and the spectra obtained are shown in panels (d), (g), and (e) respectively. For comparison, panel (f) shows spectra from literature of laboratory-generated soot coated by α-pinene (in red) and naphthalene SOA (in black) [2]. We did not observe similar peak features between 285 and 300 eV, but find peaks corresponding to K^+ (296 eV), sulfate (170-180 eV) and calcium (345-350 eV), suggesting that this particular particle examined most likely originates from mineral dust. Other particles in the same sample show indicators of different origins, comprising carbon, nitrogen, or heavy metal peaks. Detailed analysis is required for more accurate conclusions. Chemical mapping of single particles is still extremely rare, and these experiments give a first glimpse into the heterogeneity of samples previously assumed to be uniform.

Laboratory-generated samples were mapped with focus on spatially resolved chemical characterization. Detailed analysis will reveal presence of biases in sampling procedures.

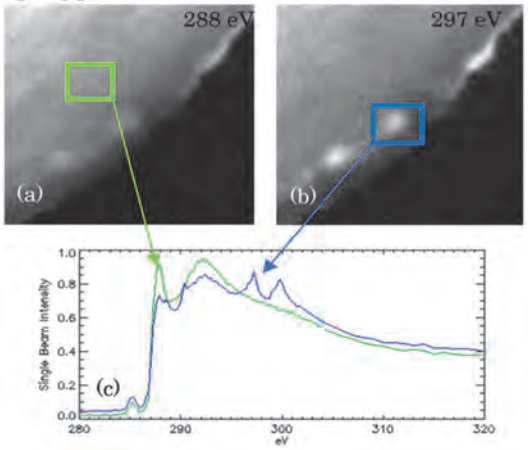

Fig. 1. Optical density of plastic sample at various photon energies. Bright areas indicate where excited functional groups are located. (a) Regions with C-C bonds; (b) Presence of K; (c) Spectra obtained from selected regions showing peaks corresponding to of C-C (288 eV), C=C (285 eV), and K (296 eV).

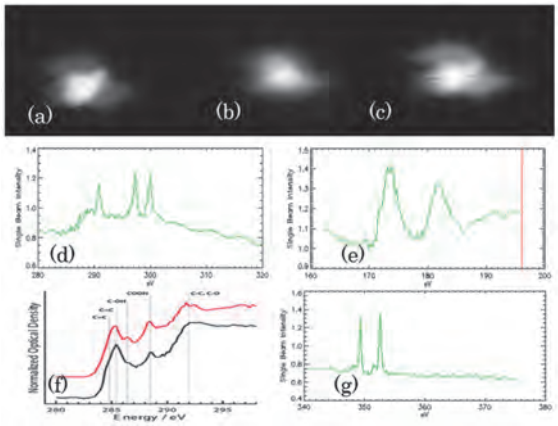

Fig. 2. Urban aerosol at different absorption edges and literature reference of organic aerosol absorption spectra.

[1] R. C. Moffet, A.V. Tivanski and M.K. Gilles, Fundamentals and Applications in Aerosol Spectroscopy (CRC Press; Boca Raton, Fl, 2011).
[2] J. C. Charnawskas *et al.*, Faraday Discussions **200** (2017) 165.

BL4U

STXM-XANES Analysis of Carbonaceous Matter of the Ediacara Biota-type Fossils from the Early Cambrian Chengjiang Section

T. Komiya[1], T. Ohigashi[2,3], D. Shu[4], J. F. H. Cuthill[5,6] and J. Han[4]

[1]*Department of Earth Science and Astronomy, The University of Tokyo, Meguro 153-8902, Japan*
[2]*UVSOR Synchrotron Facility, Institute for Molecular Science, Okazaki 444-8585, Japan*
[3]*School of Physical Sciences, The Graduate University for Advanced Studies (SOKENDAI), Okazaki 444-8585, Japan*
[4]*Early Life Institute & Department of Geology, Northwest University, 229 Taibai Road, Xi'an 710069, P.R. China*
[5]*Earth-Life Science Institute, Tokyo Institute of Technology, Tokyo 152-8550, Japan.*
[6]*Department of Earth Sciences, University of Cambridge, Downing Street, Cambridge, CB2 3EQ, UK*

The Ediacara biota is one of the enigmatic organism groups through geologic history. The biota occurred in the late Ediacaran from 580 to 543 Ma, namely during the early evolution of the Metazoan. Their sizes and complexity indicate that they should be multi-cellular animals, but it is still controversial which phylum/phyla the Ediacara biota belong to. Seilacher (1989) proposed a new stem group of Vendobionta, independent of all living-Metazoa. On the other hand, recent reappraisals suggest that each organism of the Ediacaran biota should belong to a stem group of each closely-related phylum of the living organisms (e.g. Xiao & Laflamme, 2009). Because some of the biota have similar morphology to extant cnidarians and molluscs, their classification into the phyla is plausible, but most of them have quite different morphology from the extant and even extinct Metazoa; thus the identification does not work for most of them.

Generally speaking, each organism has its own organic molecules, related to the function, such as chitin and hemocyanin for arthropods and molluscs. Therefore, detection of the unique organic molecules is useful to identify the precursor organisms of the fossils. We tried detecting the organic molecules from carbonaceous matter (CM) in four Ediacara biota-type fossils from the Chengjiang area, South China.

The C-K X-ray absorption near edge structure (XANES) spectra of the CM were acquired using a scanning transmission X-ray microscope (STXM) at the BL4U, UVSOR. Raman microspectroscopic analysis on the fossils was performed in order to identify the CM before the XANES analyses.

Figure 1A shows four analytical points on an STXM image of the Sample 4. Figure 1B shows C-XANES spectra of the CM in the Sample 4 along with typical spectra of chitin and collagen. The spectra are different among the analytical points, suggesting that the CM is heterogeneous. The Chitin has two distinguished peaks at 285.1 and 288.56. The spectra of the sample 4, as well as other samples 1–3, are dissimilar to those of chitin and collagen. The absorption peaks around 285 eV and at 292 eV possibly correspond to 1s to π* of electronic transitions in aromatic C=C bonds, and 1s to σ* exciton of graphite, respectively, which are typical for graphitized carbon.

This study can detect neither chitin nor collagen from the Ediacara Biota-type fossils from South China. Analysis of better-preserved specimen is required to identify the precursor organisms from the fossils.

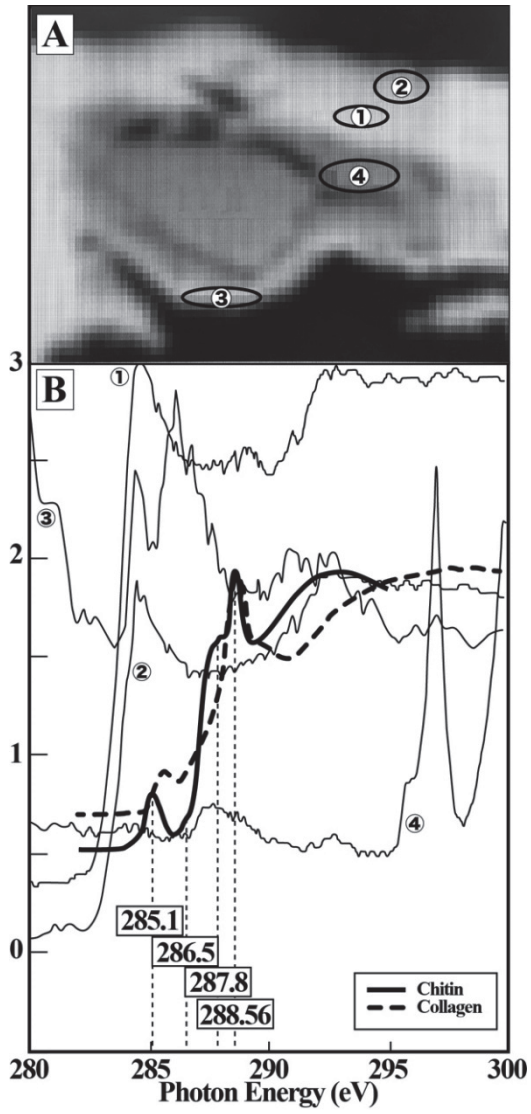

Fig. 1. (A) Analytical points on Sample 4. (B) Carbon-XANES spectra of the analytical points on the Sample 4 (A), and organic molecules of chitin and collagen.

BL4B

Preliminary Study on Nitrogen K-edge XANES on Martian Meteorites

R. Nakada[1] and M. Koike[2]

[1]*Kochi Institute for Core Sample Research, Japan Agency for Marine-Earth Science and Technology (JAMSTEC), Nankoku 783-8502, Japan*

[2]*Institute of Space and Astronautical Science (ISAS), Japan Aerospace Exploration Agency (JAXA), Sagamihara 252-5210, Japan*

Surface environment of terrestrial planet varies to a large degree. The understanding on the diversity and universal property of planetary surface environment is one of the most important study for the planetary science and is related to the habitability. Volatile elements such as hydrogen, carbon, and nitrogen circulate through inner and surface of a planet and determine the evolution of the planetary environment. However, the behavior and cycles of volatile elements in the other planet than the Earth is largely unknown. Mars had experienced a great environmental change; it held a large body of liquid water on the surface in ~4 billion years ago, while presents a cold and dry environment today [1]. This study focuses on the nitrogen on Mars and examines species and stable isotope ratio (ratio between ^{15}N and ^{14}N) of nitrogen in the Martian surface environment by analyzing the Martian meteorites.

In general, nitrogen in the planetary surface circulates through (i) atmosphere, (ii) rocks, water, and biosphere, and (iii) planetary interior by changing its species. Modern atmospheric nitrogen (N_2) on Mars is 0.15 mbar, though its $^{15}N/^{14}N$ ratio 1.6 times heavier than the atmospheric N_2 on the Earth [2]. Such a thin and heavy N_2 can be a result of the atmospheric escape. A model calculation suggests that the Mars had a dense atmosphere in the past [3]. On the other hand, recent exploration reported the presence of nitrate on the Martian surface [4]. Destructive analyses on impact melt glass of Martian meteorites showed the presence of nitrate with the remarkably lighter $^{15}N/^{14}N$ ratios than Martian atmosphere [5, 6]. These studies suggest the importance of the nitrogen fixation on Martian surface environments. It is necessary to determine the $^{15}N/^{14}N$ ratios of individual nitrogen species to understand the Martian nitrogen cycle. However, nitrogen abundance in Martian meteorites is typically around 10 ppm [7, 8], which might be difficult to determine the nitrogen species by X-ray absorption near edge structure (XANES) analysis.

We have performed preliminary study on nitrogen K-edge (402 eV) XANES measurements on Martian meteorite at BL4B of UVSOR. $NaNO_3$ and NH_4Cl reagents were measured in total electron yield mode, while meteorites and epoxy resin were measured in fluorescence mode.

Small but clear X-ray absorption was observed for some samples (Fig. 1). However, it should also be noted that nitrogen X-ray absorption also occurs for epoxy resin, which is generally used to make thin section of a meteorite. In contrast, any absorption was observed from indium which is also used for sample mounting. Regarding the nitrogen K-edge XANES spectra of Martian meteorites, possible contribution of contaminant during preparation procedure should be checked in future.

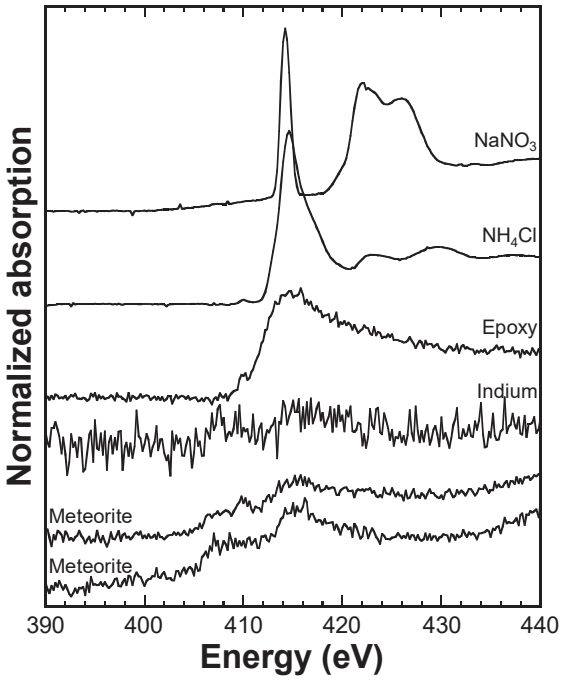

Fig. 1. Nitrogen K-edge XANES spectra of standards and samples.

[1] V. R. Baker, Nature **412** (2001) 228.
[2] M. H. Wong *et al*., Geophys. Res. Lett. **40** (2013) 6033.
[3] H. Kurokawa *et al*., Icarus **299** (2018) 443.
[4] J. C. Stern *et al*., PNAS **112** (2015) 4245.
[5] M. M. Grady *et al*., J. Geophys. Res. **100** (1995) 5449.
[6] S. P. Kounaves *et al*., Icarus **229** (2014) 206.
[7] Y. N. Miura *et al*., GCA **59** (1995) 2105.
[8] K. Mathew and K. Marti, J. Geophys. Res. **106** (2001) 1401.

BL5B

Evaluation of the Hydrogen Absorption Cell Imager for Planetary Explorations

M. Kuwabara[1], M. Taguchi[2], K. Yoshioka[3], T. D. Kawahara[4], S. Kameda[2], S. Komoriya[2], S. Yonemoto[3], Y. Shirafuji[2] and S. Kawase[2]

[1]*Institute of Space and Astronautical Science, Japan Aerospace Exploration Agency, Sagamihara 252-5210, Japan*
[2]*College of Science, Rikkyo University, Tokyo 171-8501, Japan*
[3]*Graduate School of Frontier Sciences, The University of Tokyo, Chiba 277-8561, Japan*
[4]*Faculty of Engineering, Shinshu University, Nagano 380-8553, Japan*

In the planetary lower atmosphere, H_2O generate mainly hydrogen atoms through photodissociation by sunlight. The generated hydrogen atoms ascend to the exopause and only those atoms which have higher kinetic energy than gravitational potential energy there escape to interplanetary through thermal dissipation. Understanding the dissipation process in the present environment gives us some information to estimate planetary atmospheric evolution.

Hydrogen atoms in the planetary exosphere resonantly scatter the solar H Lyman-alpha radiation (121.567 nm) and form the planetary hydrogen corona. Imaging of this emission gives us to obtain the spatial structure of the corona because its brightness depends on the number density of the hydrogen atoms.

An absorption cell technique is efficient for remote sensing for the density and temperature distributions of the exospheric hydrogen atoms in the planet. In addition, the absorption cell technique has some advantages over others from the point of view of geometrical size, weight, simplicity, and durability. Thus, the technique is suitable for future missions with small size spacecraft.

An absorption cell photometer was mounted on the first Japanese Mars mission [1, 2], NOZOMI, but the parameter optimization for the absorption cell was insufficient due to the limitation of the development time. Therefore, further optimization and study have been required for future space missions. We evaluated the performances which depend on filament shape, applied power to the filament, enclosed gas pressure, optical path length of the cell, and position of the incident light using an ultra high resolution Fourier transform spectrometer installed on the DESIRS beamline of Synchrotron SOLEIL in France in 2016 and 2018. However, additional evaluations of the performances, such as an endurance test of the filaments, confirmation of absorption stability, have been needed. See *Kuwabara et al.* [2018] for more details [3].

In this experiment, we evaluate the stability of the absorption performance of the cell using the SOR beam with high intensity and stability. Figure 1 shows the configuration of the experiment. A prototype of hydrogen absorption cell imager consists of an absorption cell, MgF_2 band-pass filter, and photon detector. Microchannel plates and a resistive anode encoder are assembled and used as the photon detector. The absorptance of the cell for the hydrogen Lyman-alpha radiation (121.567 nm) is measured with a repeat of turning on and off filaments at 0.3 Hz through approximately 60 hours.

The result is shown in Fig. 2. The absorptance seems to be stable and its value is 4.95% ± 0.92. The errors are caused by the measurement system. For the next step, further long-term stability should be investigated.

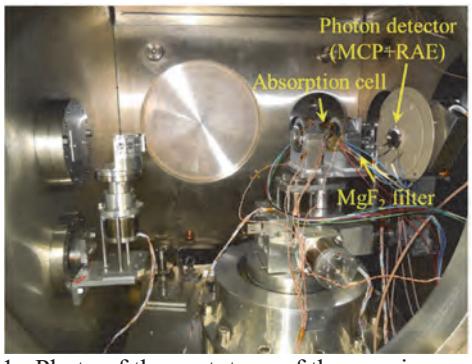

Fig. 1. Photo of the prototype of the new imager.

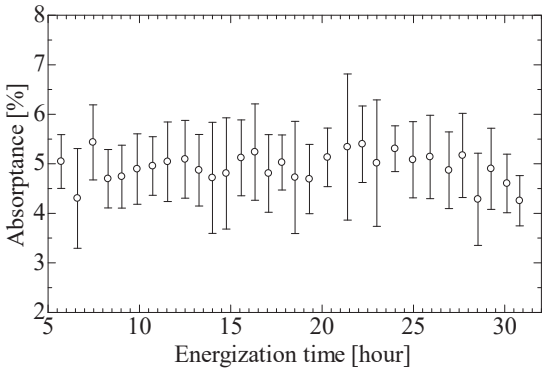

Fig. 2. Temporal variation of the absorptance of the prototype of the new imager.

[1] T. D. Kawahara *et al.*, Applied Optics **36** (1997) 2229.
[2] M. Taguchi *et al.*, Earth, Planets and Space **52** (2000) 49.
[3] M. Kuwabara *et al.*, Rev. Sci. Instrum. **89** (2018) 023111.

BL7B

Effect of Space Weathering on Identification of Organic Matter on Celestial Body Surface Using Ultraviolet Wavelength Region Spectrum

S. Arao[1], I. Yoshikawa[1,2], K. Yoshioka[1,2], I. Sakon[3], R. Hikida[1], R. Katsuse[2] and I. Endo[3]

[1]*Department of Earth and Planetary Science, Graduate School of Science, The University of Tokyo, Tokyo 113-0033, Japan*

[2]*Department of Complexity Science and Engineering, Graduate School of Frontier Sciences, The University of Tokyo, Chiba 277-8561, Japan*

[3]*Department of Astronomy, Graduate School of Science, The University of Tokyo, Tokyo 113-0033, Japan*

Analysis of reflection spectrum is a conventional means for identifying compositions of the celestial body's surface, but in the ultraviolet region, it has rarely been conducted. Analysis of spectrum suggests the existence of polycyclic aromatic hydrocarbon (PAH) in interstellar dust and on the surface of Mars' moon Phobos, but the replication study is insufficient. A comparison of the spectra of natural terrestrial PAH mixtures with that of interstellar dust or the Phobos surface suggests that there are similarly shaped absorption bands around wavelengths of 210 nm and 217.5 nm respectively. This similarity is the basis of the hypothesis that PAH is present in interstellar dust and the Phobos surface. However, considering the gap of peak wavelength, there are also many negative opinions on the hypothesis. Thus, there has been no definitive conclusion until now.

One of the phenomena that may have a description for this problem is change in the absorption spectrum due to space weathering. The absorption band of PAH around the wavelength of 210 nm is caused by the transition of aromatic π electrons and their orbital area relates to the absorption peak wavelength. If the hydrogen atoms bonded to the aromatic rings of PAH molecules are desorbed by space weathering, it is suggested theoretically that the orbital area of aromatic π electrons is broadened and the absorption band's peak wavelength may approach 217.5 nm.

In this experiment, to evaluate the influence of space weathering on the optical properties of PAH, we prepared several PAH (coronene and chrysene) samples which had been exposed to the space environment for about 1 year on orbit of the International Space Station (ISS). Then, we compared the reflection characteristics of these samples with those of non-exposure samples in a wavelength region of 160-300 nm.

As a result, all the samples experienced space weathering reflected the light in 160-300 nm wavelength region more weekly than non-exposure samples did. Furthermore, reflection characteristics of coronene sample exhibited a broad dip around 235 nm wavelength and showed a trend in 210-280 nm wavelength region that the attenuation of the reflected light is more significantly at longer wavelengths (Fig. 1). This trend suggests that the wavelength which corresponds to the bottom of the dip may shift to the direction of longer wavelength due to space weathering.

As another research, to detect the main factor of space weathering, we are going to irradiate non-exposure PAH samples with UV light or radial ray simulating the environment on the flight orbit of the ISS, and compare their reflection characteristics with those of space weathered sample.

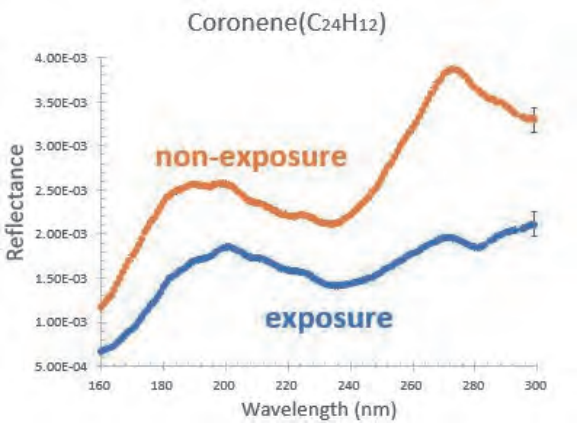

Fig. 1. Reflection characteristics of coronene sample in a wavelength region of 160-300 nm. Each curve shows an average of measured values upon three different incident points on the sample. Typical errors are added on the plots at 300 nm wavelength.

[1] Bertaux *et al*., Proceedings of the EPSC-DPS Joint Meeting. 2011.
[2] Hendrix *et al.*, Meteoritics & Planetary Science **51** (2016) 105.
[3] Joblin *et al*., The Astrophysical Journal **393** (1992) L79.
[4] Sakata *et al*., Nature **301** (1983) 493.
[5] Steglich *et al*., The Astrophysical Journal **742** (2011) 2.

UVSOR User 7

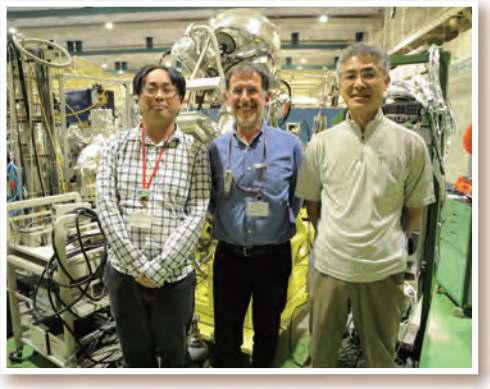

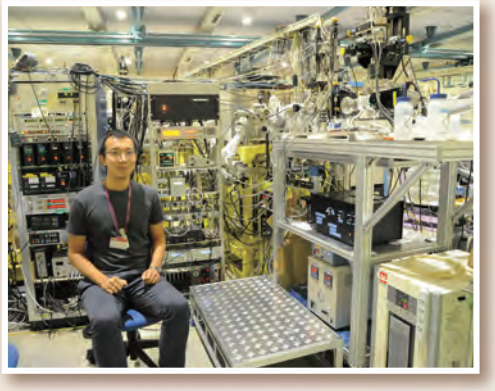

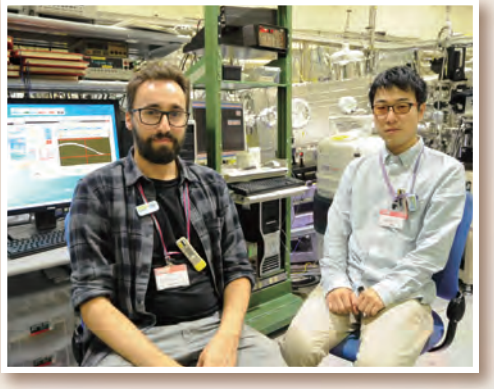

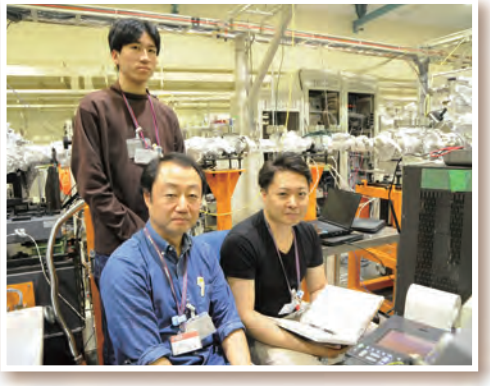

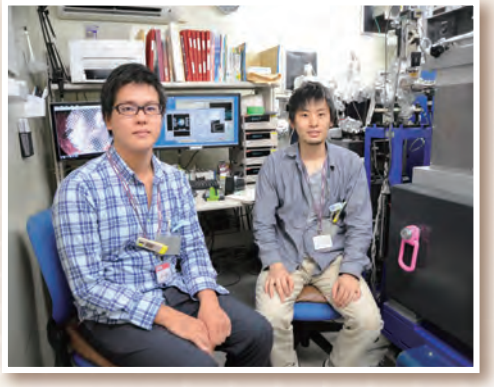

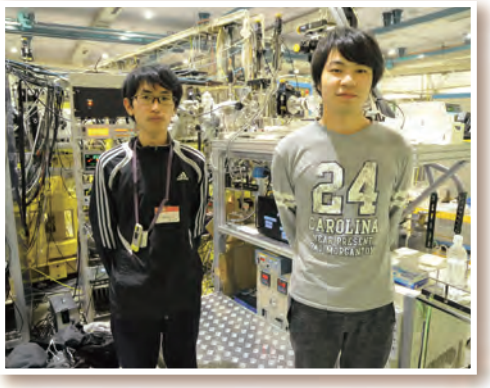

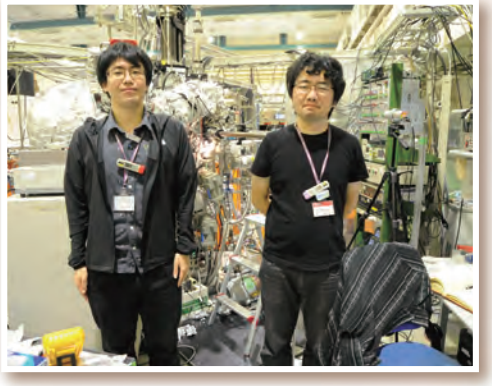

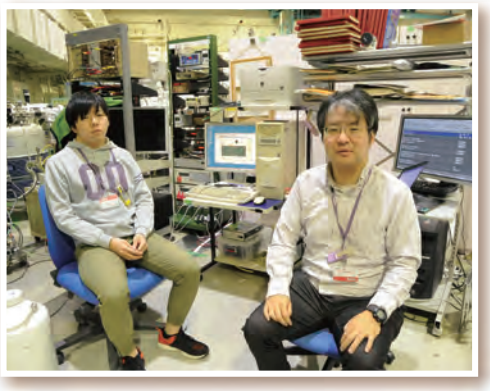

UVSOR User 8